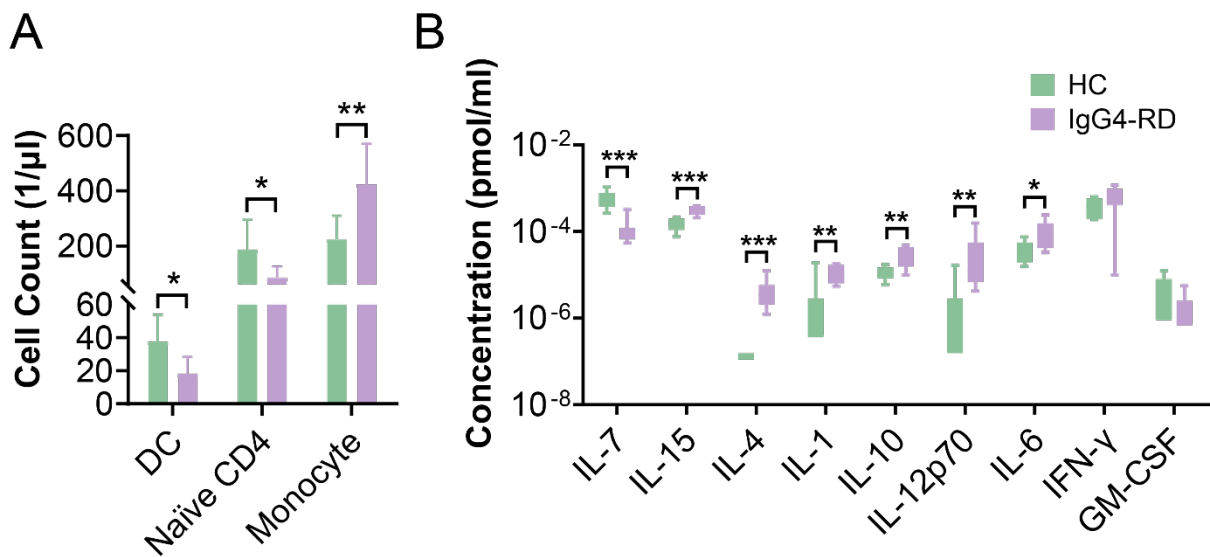
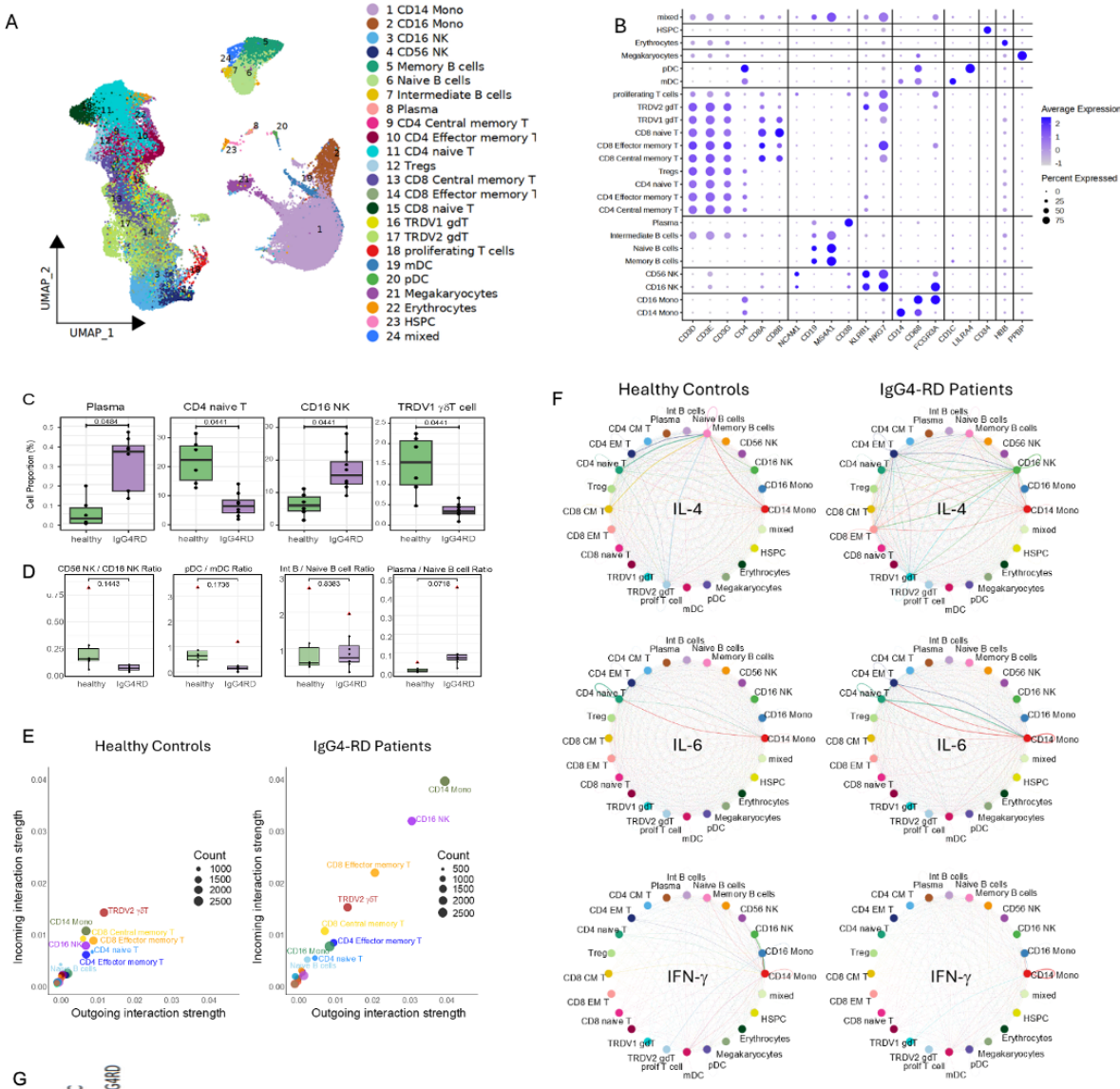


1 **Figure 1. Study design.** Peripheral blood samples were collected from IgG4-RD
 2 patients and healthy controls, measured by flow cytometry for cell type abundances,
 3 MSD immunoassays for cytokine levels, and single-cell RNA sequencing for single-
 4 cell transcriptome. These multi-omic measurements, along with the established IgG4-
 5 RD and immunological knowledge, were integrated for mechanistic modeling of IgG4-
 6 RD, on which *in silico* perturbations were conducted to identify potential drug targets
 7 and evaluate therapeutic effects. This figure was generated via biorender:
 8 www.biorender.com

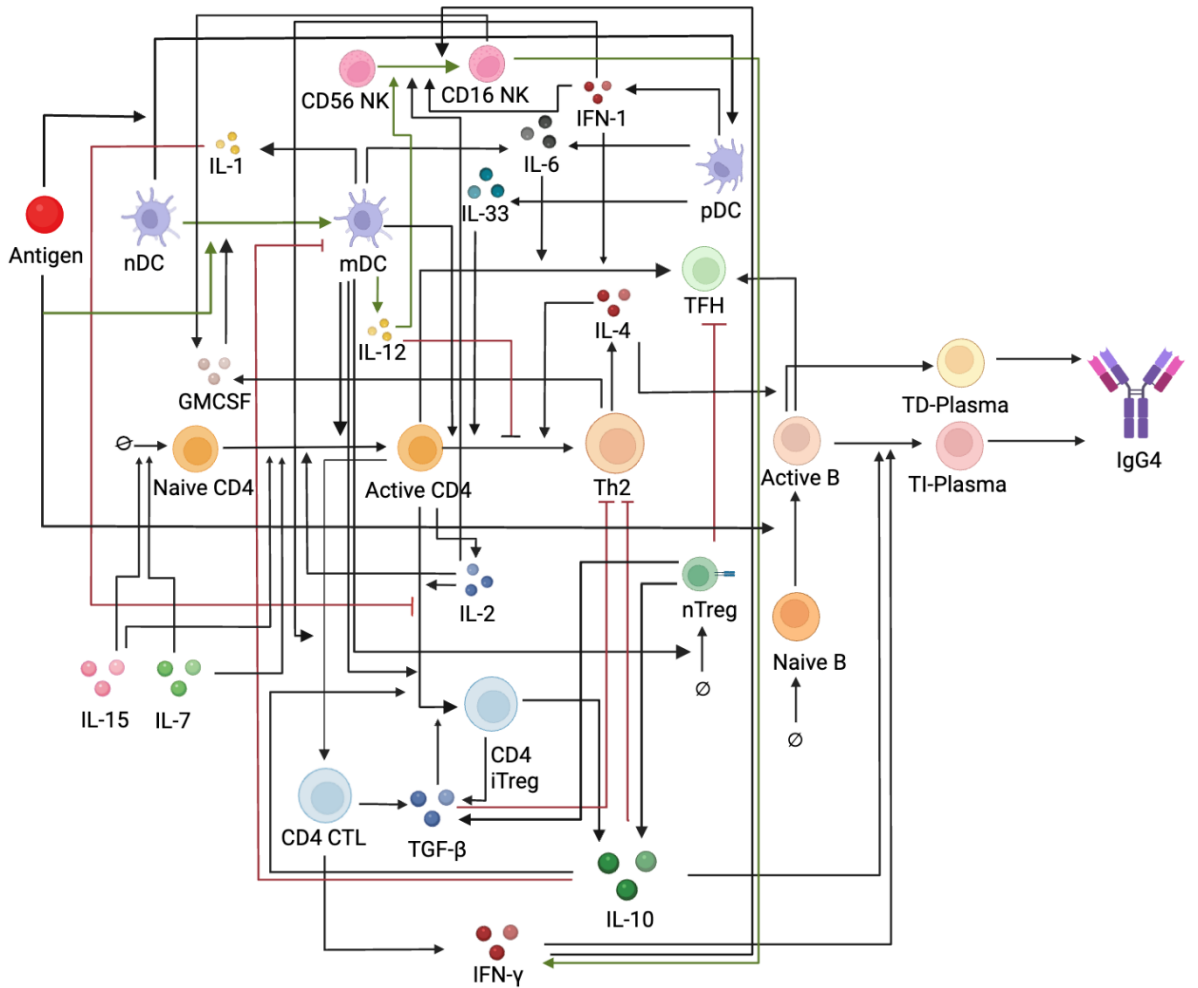


9

10 **Figure 2. Measured changes of circulating immune cells and cytokines in IgG4-**
11 **RD. (A) Cell types significantly changed in cell number (normalized to total cells/ μ L)**
12 **between the healthy controls and the IgG4-RD patients, measured by flow cytometry.**
13 **(B) Changes in serum cytokine levels (pmol/mL) between the controls and the**
14 **patients, measured by MSD proteomics platform. * $P<0.05$, ** $P<0.01$, *** $P<0.005$**



15 **Figure 3. scRNA sequencing revealed alterations in cell abundance, gene
16 expression, and cell-cell communications in IgG4-RD.** (A) Cell type clustering and
17 annotation displayed on a uniform manifold approximation and projection (UMAP). (B)
18 Expression of cluster-specific genes. (C) Cell types with significant proportional
19 changes between the healthy controls and the IgG4-RD patients. (D) Ratio of specific
20 cell subsets: CD56/CD16 NK cells; pDC / mDC; Intermediate B/Naïve B cells;
21 Plasma/Naïve B cells. (E) Strengths of cellular signaling for the healthy controls and
22 the IgG4-RD patients. (F) The cellular signaling of IL-4, IL-6, and IFN- γ in the healthy
23 controls and the IgG4-RD patients.



24

25 **Figure 4. Network topology of the IgG4-RD disease model.** The network topology
 26 includes 16 essential immune cell types and 13 essential cytokines. Upon the
 27 recognition of self-antigens, the immune system shifts from the healthy state to the
 28 disease state through the interactions of these immune cells and cytokines. The
 29 interaction kinetics are derived by fitting ordinary differential equations into the multi-
 30 omic measurements under the maximum likelihood, resulting in 15 sets of kinetics.
 31 Black arrows: cell differentiation and cytokine secretion. Green arrows: activation.
 32 Red arrows: inhibition.

33

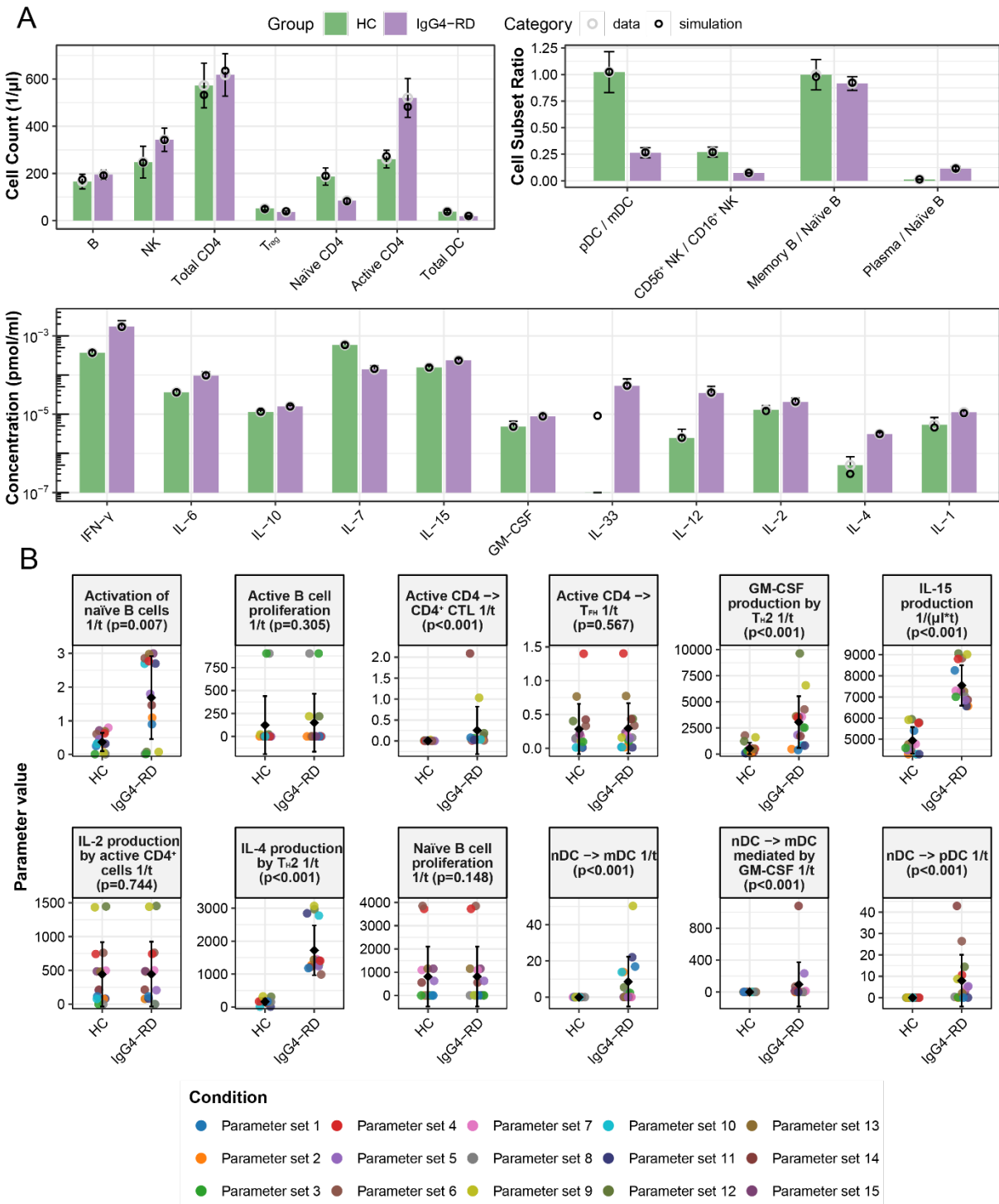
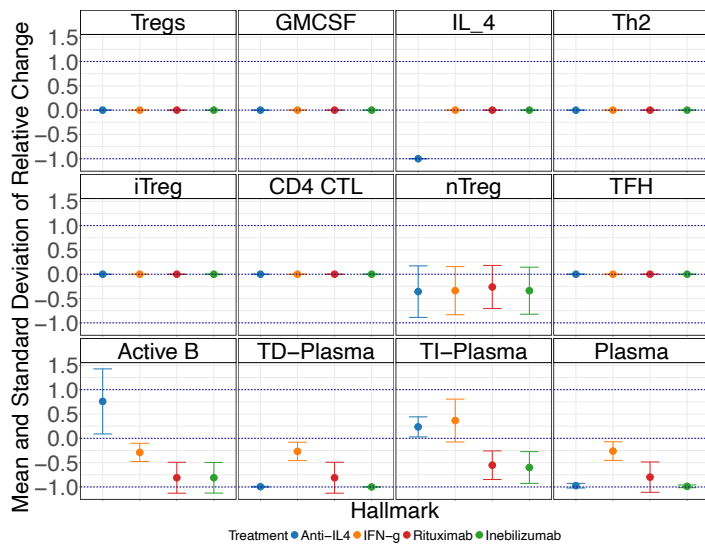


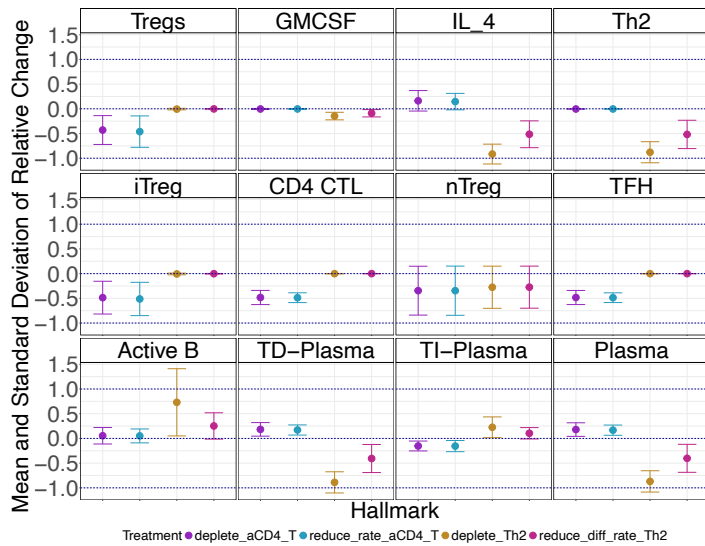
Figure 5. The IgG4-RD disease model inform changes of the immune system. (A) Fit of the IgG4-RD disease model to the data from the healthy controls (HC) and the IgG4-RD patients (IgG4D). Mean and standard deviations of the cell counts, ratios, and cytokine concentrations are plotted, with omic measurements presented in light grey and simulations across the 15 calibrated instances of the model presented in black. IL-

41 33 was only measured in IgG4-RD patients, hence the missing bar for the healthy
42 control group. **(B)** Essential immune regulation processes inferred by the calibrated
43 model for the HC and the IgG4. There are 15 calibrated instances of the model in total
44 (i.e. 15 parameter sets under the same network topology), with each dot representing
45 one model parametrization and the error bars displaying standard deviation across all
46 model parametrizations.

A



B



47 **Figure 6. *In silico* perturbation of potential therapeutic targets and resulted**
48 **changes in disease hallmarks of IgG4-RD.** Treatment effects are quantified by the
49 relative changes in the cell count or cytokine levels post-treatment compared to before-
50 treatment. Dots: mean values; error bars: standard deviations of the simulated results.
51 Fold change (FC) are displayed in log10 scale. **(A)** Effects of perturbing four targets
52 identified from our multi-omic measurements: B-cell depletion by rituximab or
53 inebilizumab, anti-IL-4, and enhancing IFN- γ . *Anti-IL4*: degradation rate of IL-4, with
54 log10(FC)=1.2; *IFN- γ* : production rate of IFN- γ , with log10(FC)=0.5; *rituximab*: death
55 rate of naïve and active B cells, with log10(FC)=3; *inebilizumab*: death rate of naïve
56 and active B cells and plasma cells, with log10(FC)=3; **(B)** Effects of perturbing TCR
57 signaling and Th2 polarization, as identified from literature and outside of our multi-
58 omic measurements. *deplete_aCD4_T*: active CD4 $^{+}$ T cell depletion, with the death rate
59 of active CD4 $^{+}$ T cells set as log10(FC)=1.8; *deplete_Th2*: Th2 cell depletion, with the

60 death rate of T_{H2} cells set as $\log_{10}(FC)=1$; *reduce_diff_rate_Th2*: T_{H2} cell
61 differentiation reduction, with the differentiation rate of active CD4+ T cells into T_{H2}
62 cells set as with $\log_{10}(FC)=-1$; *reduce_rate_aCD4_T*: suppression of CD4+ T cell
63 activation, with the activation rate of naive CD4+ T set as $\log_{10}(FC)=-1.1$.

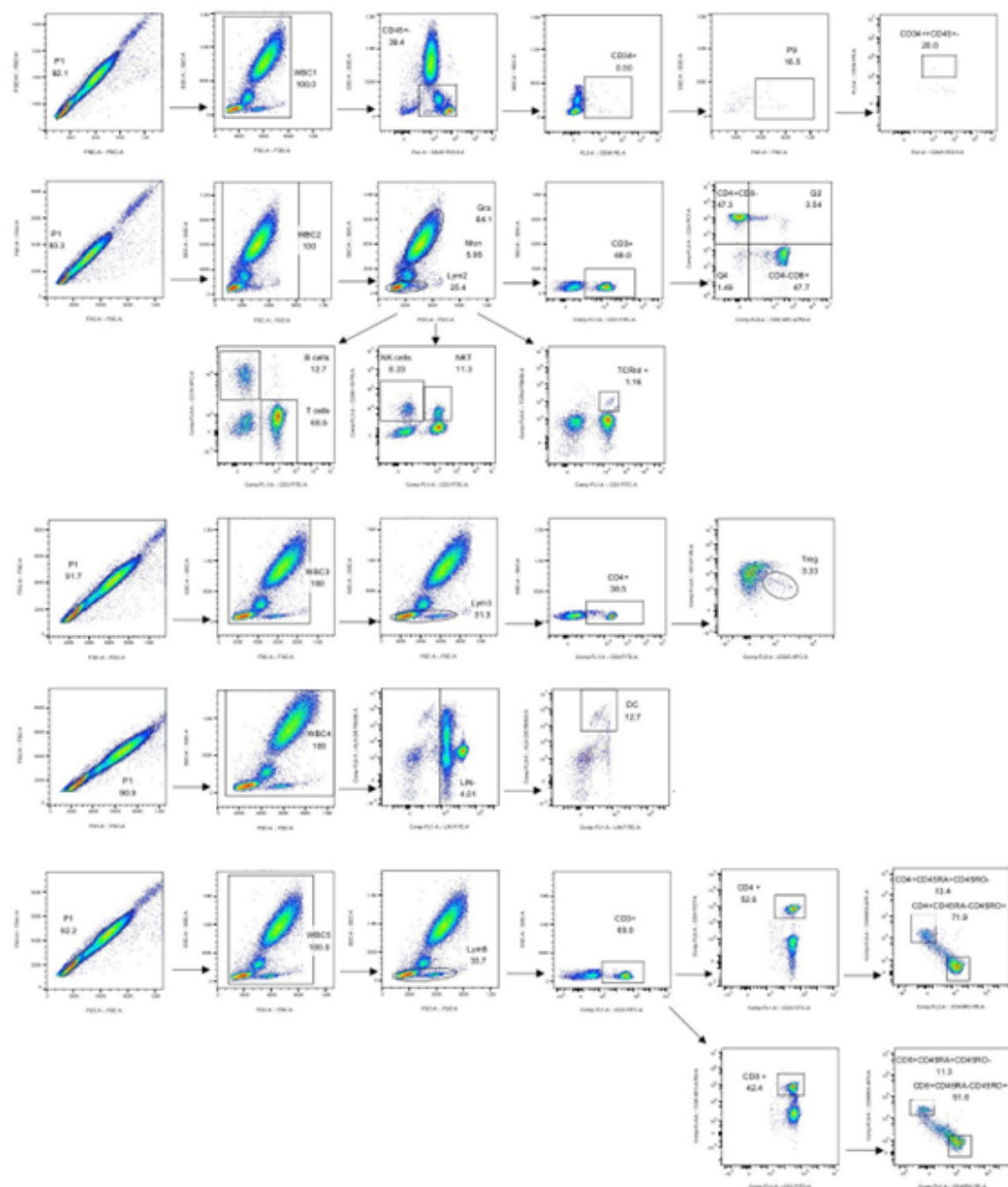
64 **Table 1. Baseline characteristics of the patients.**

65

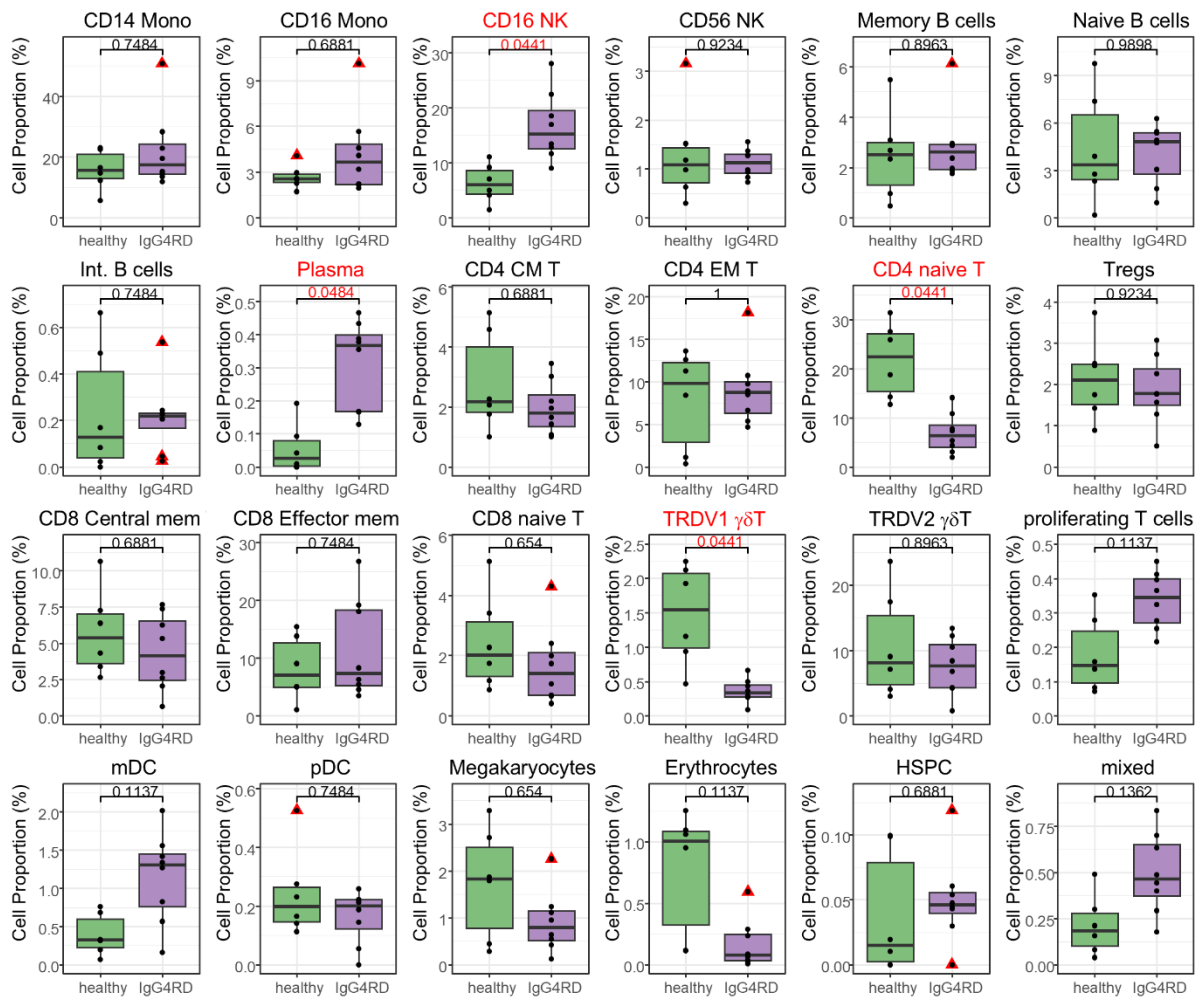
Clinical Features	Counts or lab measurements	Percentage
Sex		
Male	4	50%
Female	4	50%
Age	60.0 (48.5, 72.0)	
Symptoms		
Dry mouth and eyes	3	30%
Abdominal pain	3	30%
Weight loss	2	20%
Lacrimal gland enlargement	2	20%
Baseline Laboratory Tests		
CRP (mg/L)	1.64 (0.69, 15.72)	
ESR (mm/h)	14.50 (7.75, 61.0)	
eGFR(mL/min)	81.71 (47.63, 101.96)	
Scr (μ mol/L)	79.50 (57.50, 94.50)	
IgG4 (g/L)	17.20 (5.59, 23.38)	
IgG (g/L)	17.87 (13.67, 23.28)	
IgM (g/L)	0.830 (0.660, 0.880)	
IgE (IU/mL)	52.0 (19.42, 410.75)	
IgA (g/L)	2.07 (1.64, 2.89)	
Hemoglobin (g/L)	123 (109, 147)	

66 Lab measurements are presented in median values, followed by 25th-percentile and
 67 75th-percentile values in parenthesis.

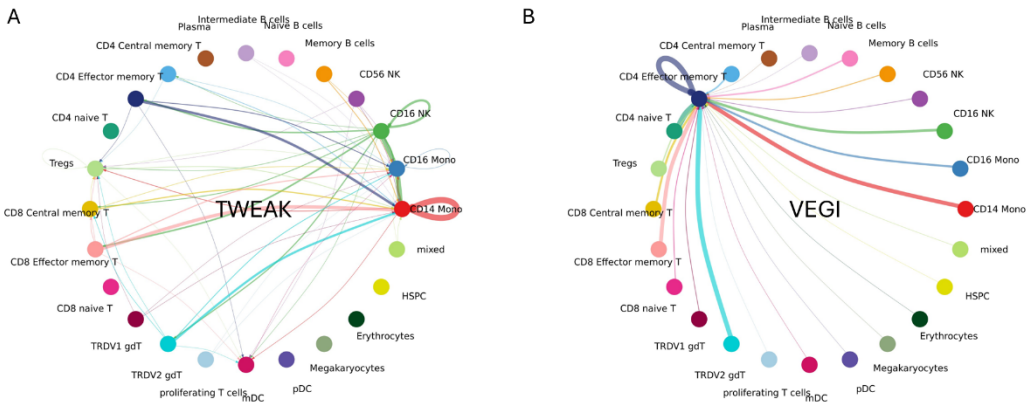
68 **SUPPLEMENTARY MATERIALS**



69 **Supplementary Figure 1:** Gating strategy for flow cytometry.

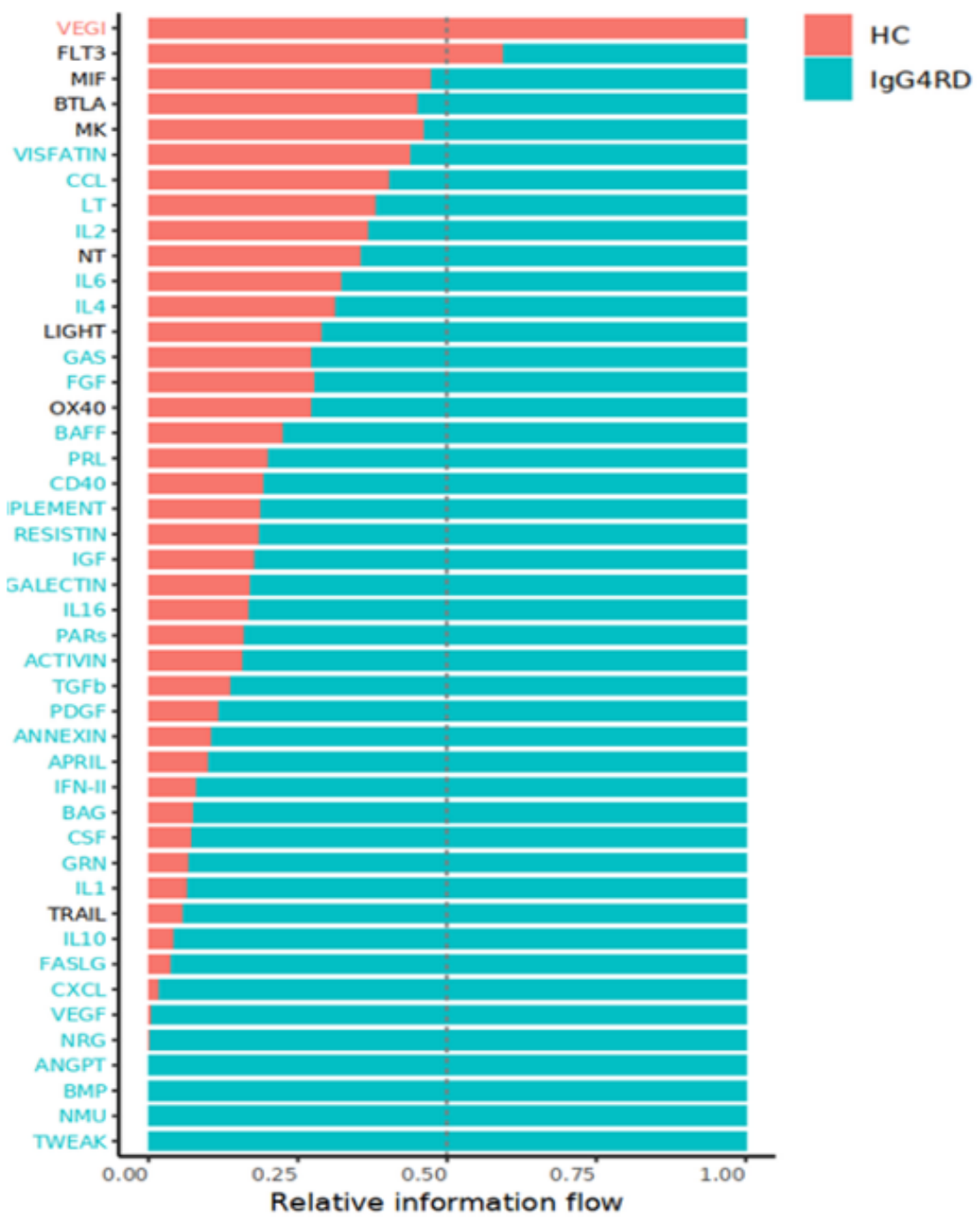


70 **Supplementary Figure 2. Overview of cell type proportions derived from scRNA**
71 **sequencing.** Significant changes ($P < 0.05$) are marked in red. Please refer to the
72 Abbreviation list for full names of the cell types. Int: Intermediate

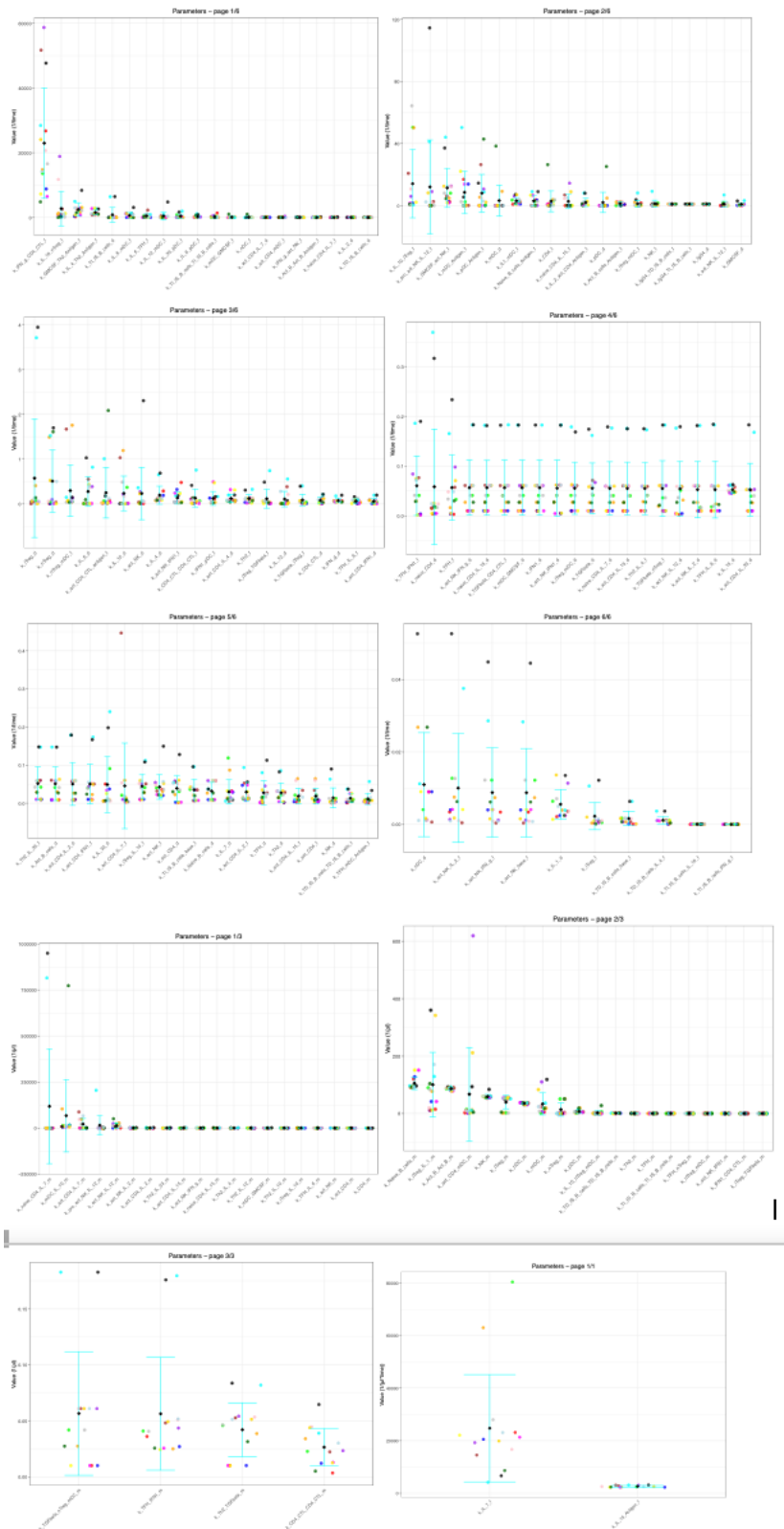


73

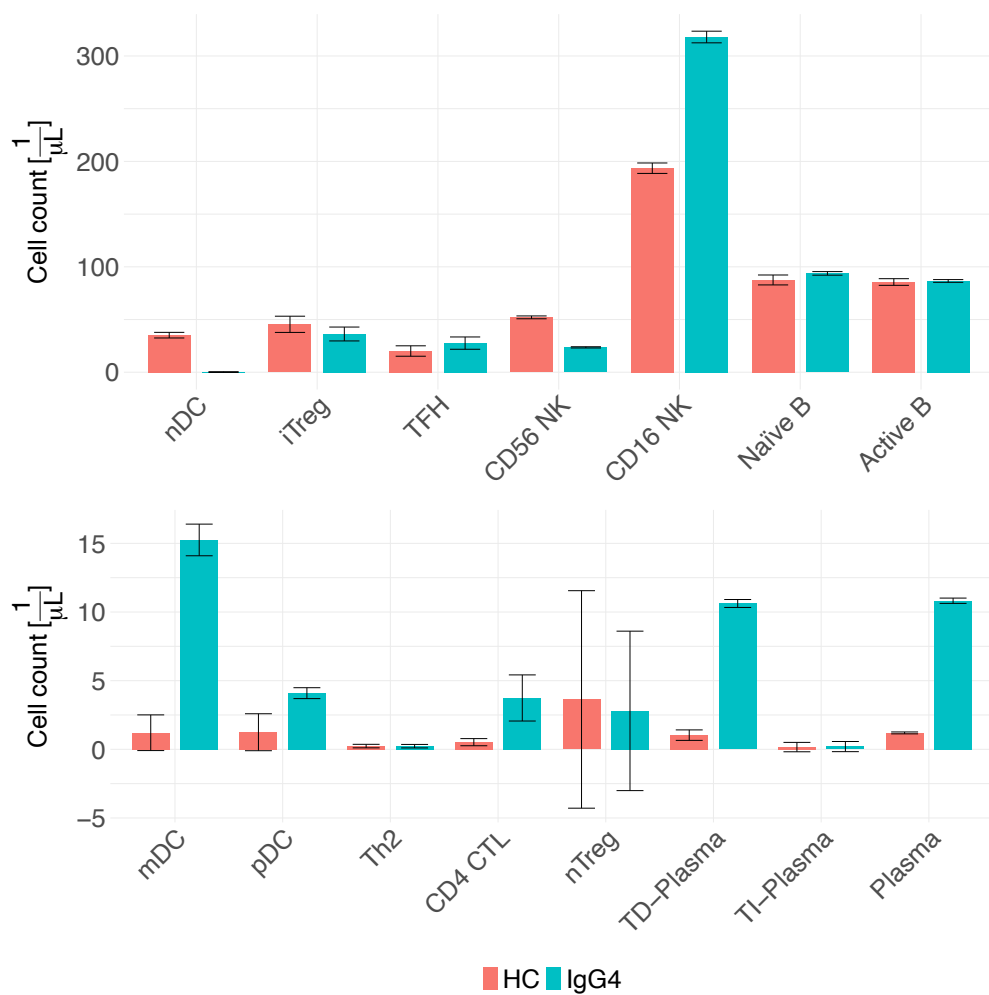
74 **Supplementary Figure 3. Cell-cell communications. (A)** TWEAK signaling
 75 specifically detected in IgG4-RD patients. **(B)** VEGI signaling specifically detected in
 76 the healthy controls.



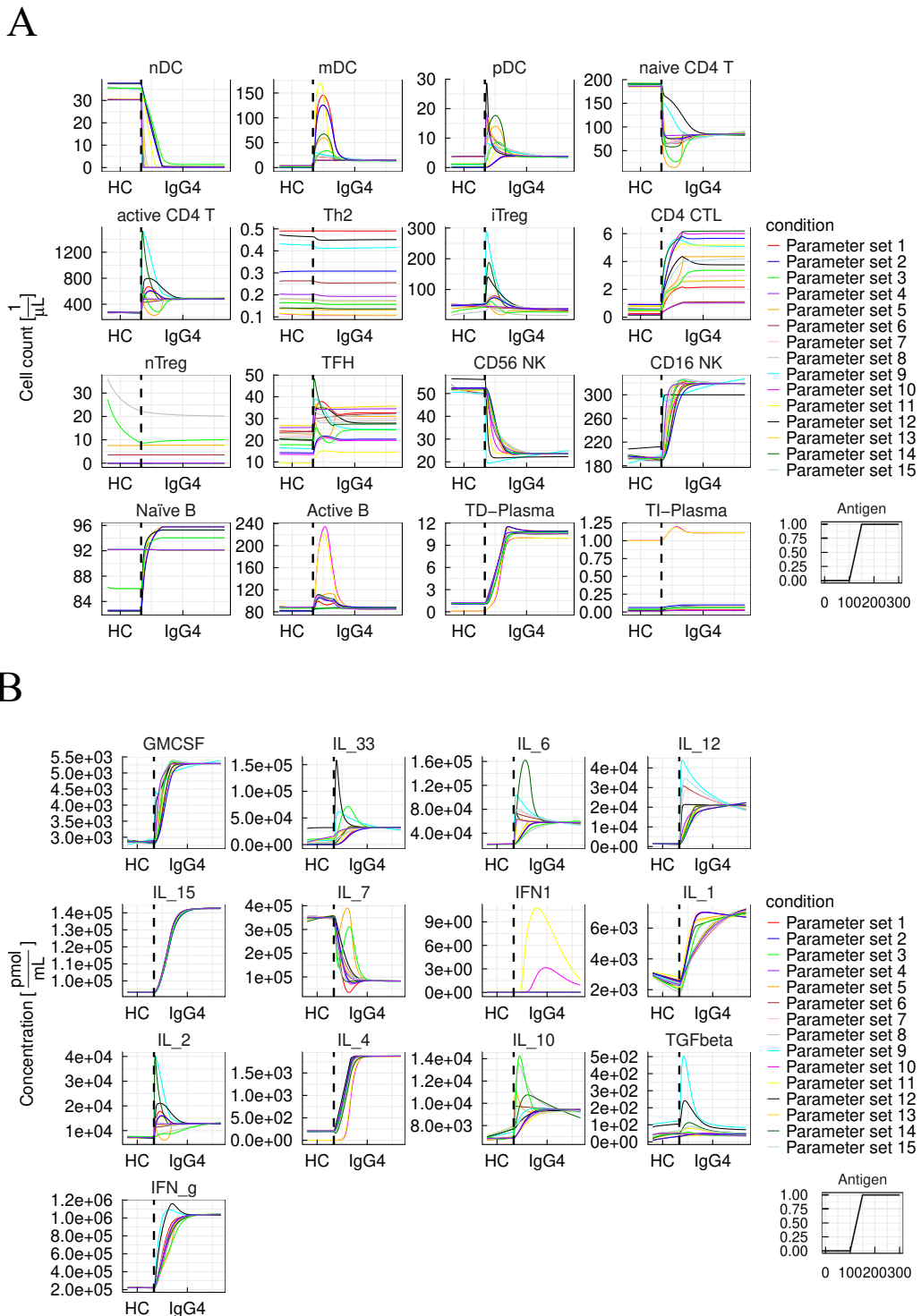
77 **Supplementary Figure 4.** Summary of the relative cellular signaling strengths between
 78 the healthy controls (HC) and the IgG4-RD patients.



79 **Supplementary Figure 5.** The distribution of estimated parameters across 15
 80 calibrated instances of the IgG4-RD model. The dots and error bars show the mean
 81 and standard deviation.

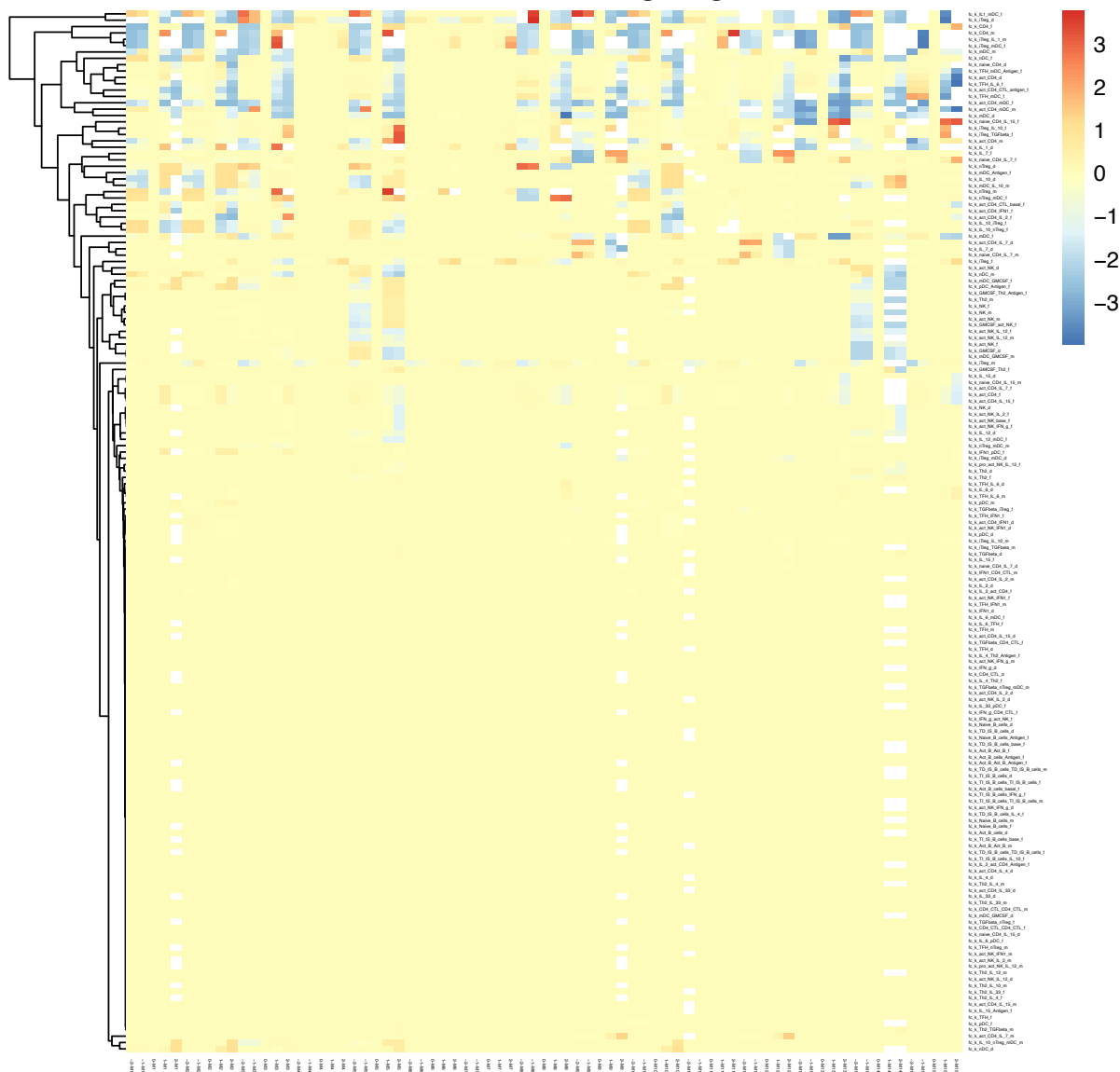


83 **Supplementary Figure 6.** The IgG4-RD disease model recapitulate multi-omic
 84 measurements in the IgG4-RD patients (IgG4) and the healthy controls (HC). The
 85 presented cell counts are simulated by the 15 calibrated instances of the model.
 86 Abbreviation list for full names of the cell types.



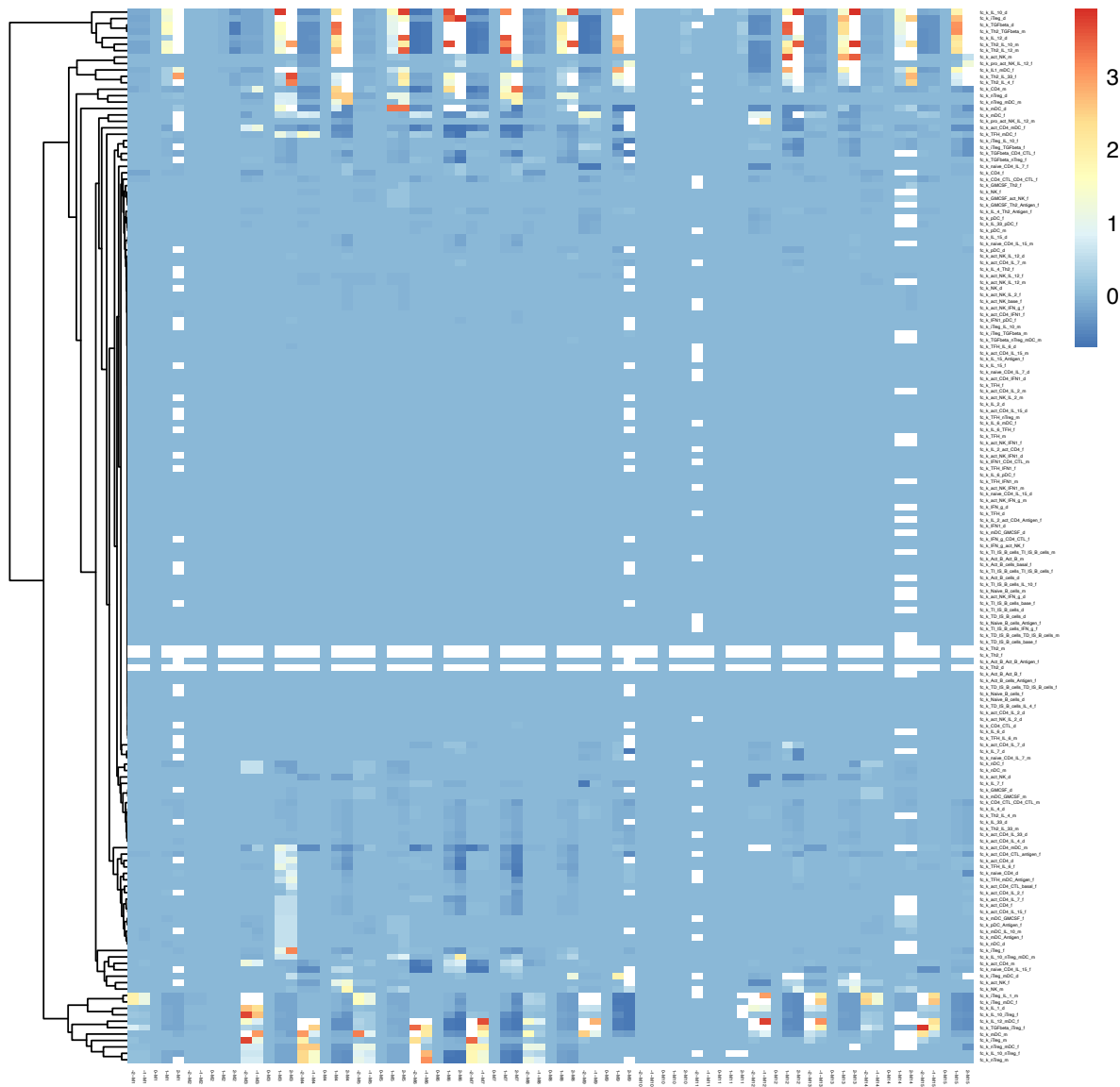
87 **Supplementary Figure 7. The simulated trajectory of immune cells and cytokines**
88 **in the IgG4-rD patients (IgG4) and the healthy controls (HC).** The 15 calibrated
89 model instances were used to simulate changes in cell counts and cytokine levels from
90 the healthy state into the disease state. Abbreviation list for full names of the cell
91 types. HC: healthy controls. IgG4RD: IgG4-RD patients.

Hierarchical clustering Tregs

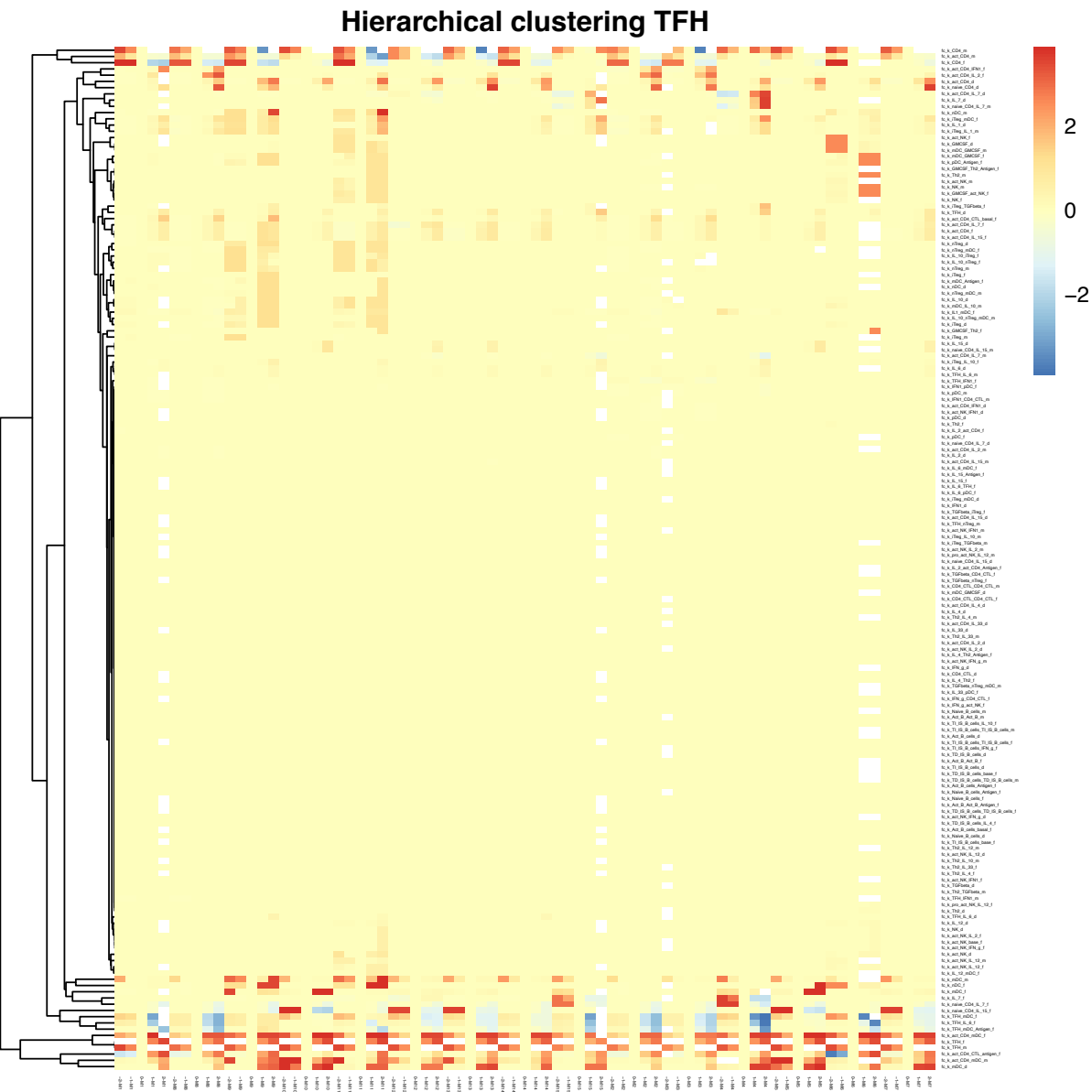


92 **Supplementary Figure 8. Sensitivity analysis of T_{reg} cells by varying model
93 parameters.** Depicted are changes in active B cell counts upon perturbing the model
94 parameters, with the change measured as $(\text{cell_count}_{\text{perturbed}} - \text{cell_count}_{\text{original}}) / \text{cell_count}_{\text{original}}$. Each row represents a model parameter. The columns show fold-
95 changes in respective parameters in each of the 15 model instances, as labeled from M1
96 to M15.
97

Hierarchical clustering Th2

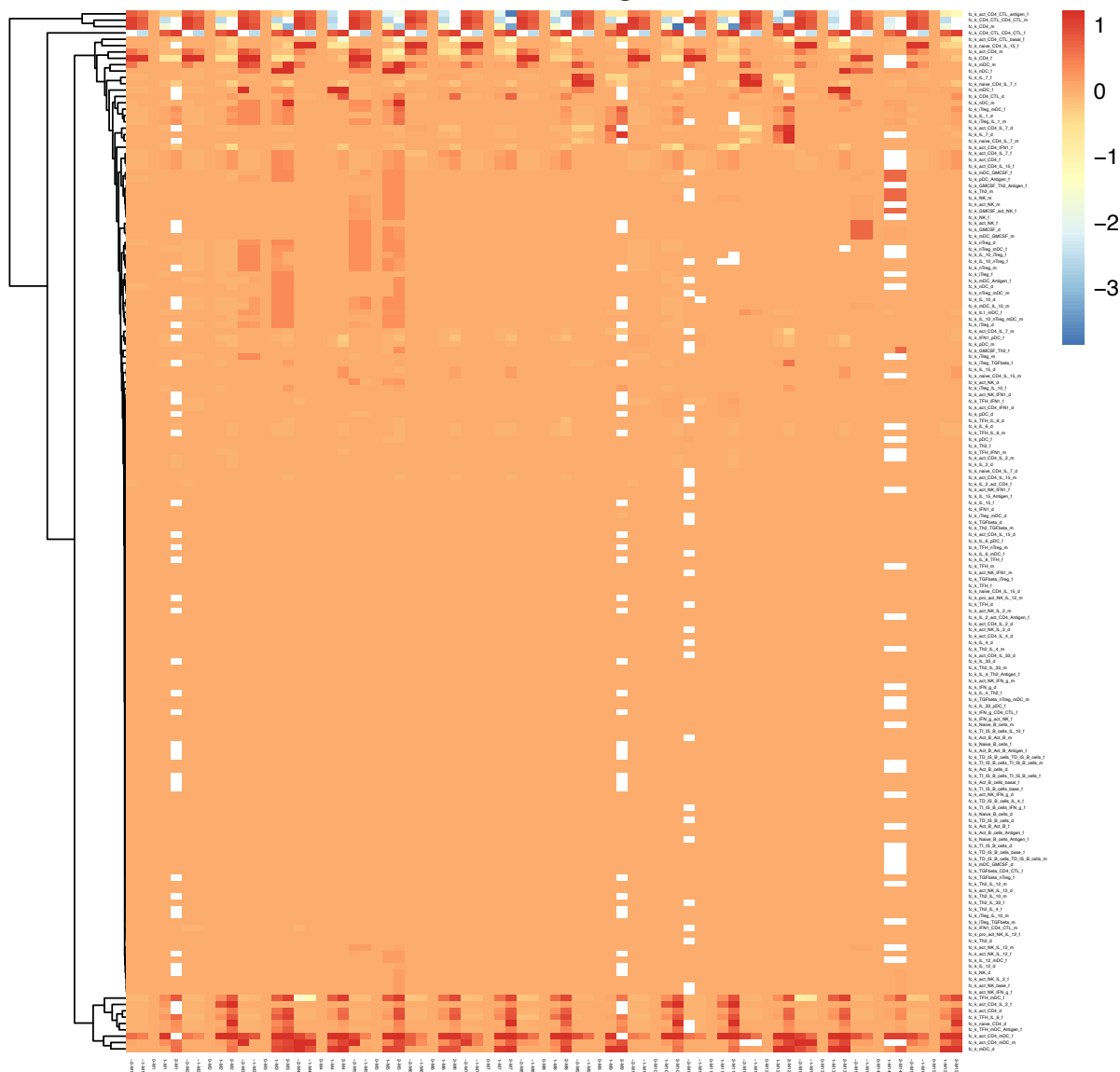


98 **Supplementary Figure 9. Sensitivity analysis of Th2 by varying model parameters.**
99 Depicted are changes in active B cell counts upon perturbing the model parameters,
100 with the change measured as $(\text{cell_count}_{\text{perturbed}} - \text{cell_count}_{\text{original}}) / \text{cell_count}_{\text{original}}$.
101 Each row represents a model parameter. The columns show fold-changes in respective
102 parameters in each of the 15 model instances, as labeled from M1 to M15.
103

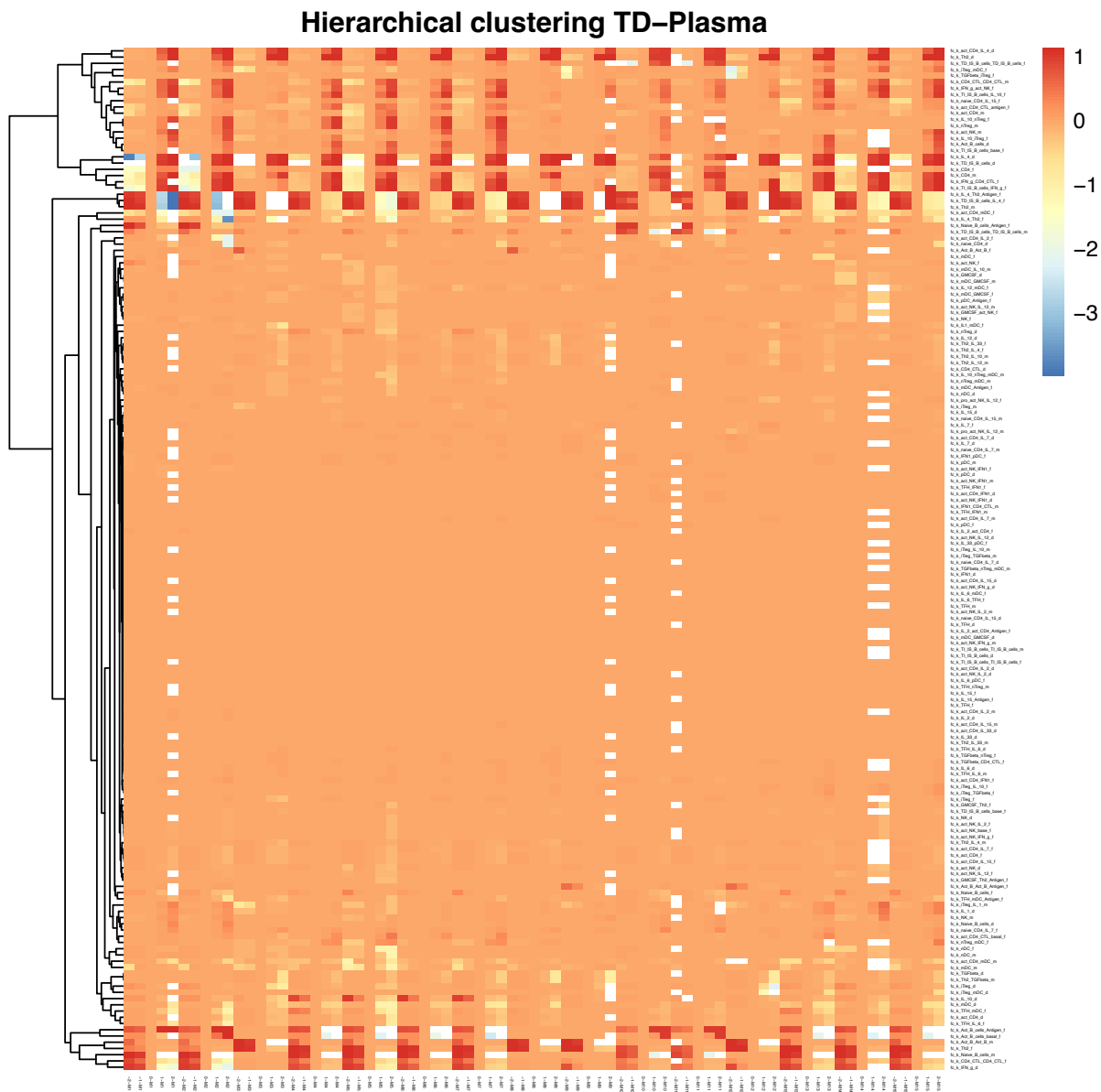


104 **Supplementary Figure 10. Sensitivity analysis of TFH Cells by varying model**
105 **parameters.** Depicted are changes in active B cell counts upon perturbing the model
106 parameters, with the change measured as $(\text{cell_count}_{\text{perturbed}} - \text{cell_count}_{\text{original}}) / \text{cell_count}_{\text{original}}$. Each row represents a model parameter. The columns show fold-
107 changes in respective parameters in each of the 15 model instances, as labeled from M1
108 to M15.

Hierarchical clustering CD4 CTL

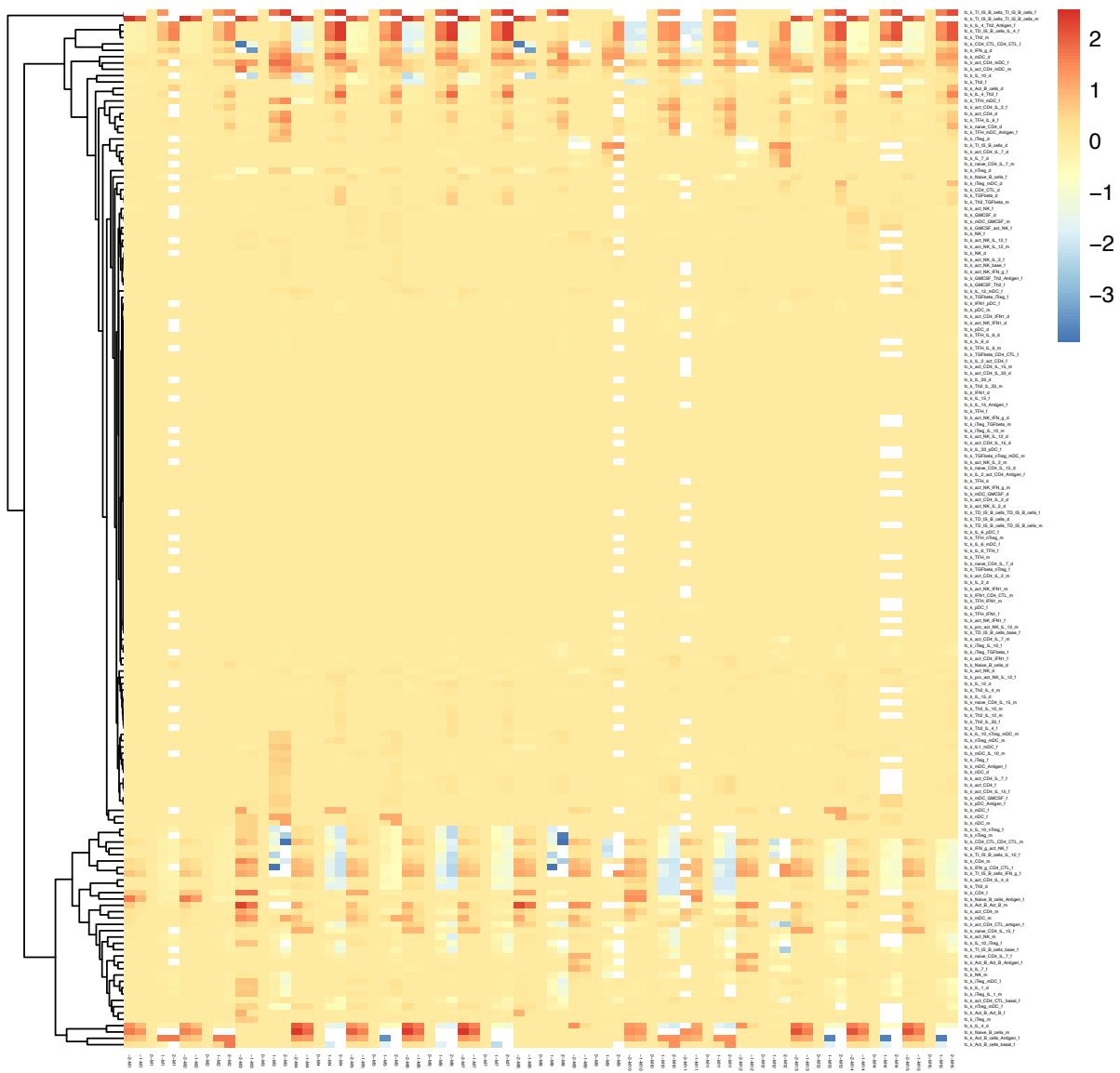


110 **Supplementary Figure 11. Sensitivity analysis of CD4⁺ CTL by varying model**
 111 **parameters.** Depicted are changes in active B cell counts upon perturbing the model
 112 parameters, with the change measured as $(\text{cell_count}_{\text{perturbed}} - \text{cell_count}_{\text{original}}) / \text{cell_count}_{\text{original}}$. Each row represents a model parameter. The columns show fold-
 113 changes in respective parameters in each of the 15 model instances, as labeled from M1
 114 to M15.
 115

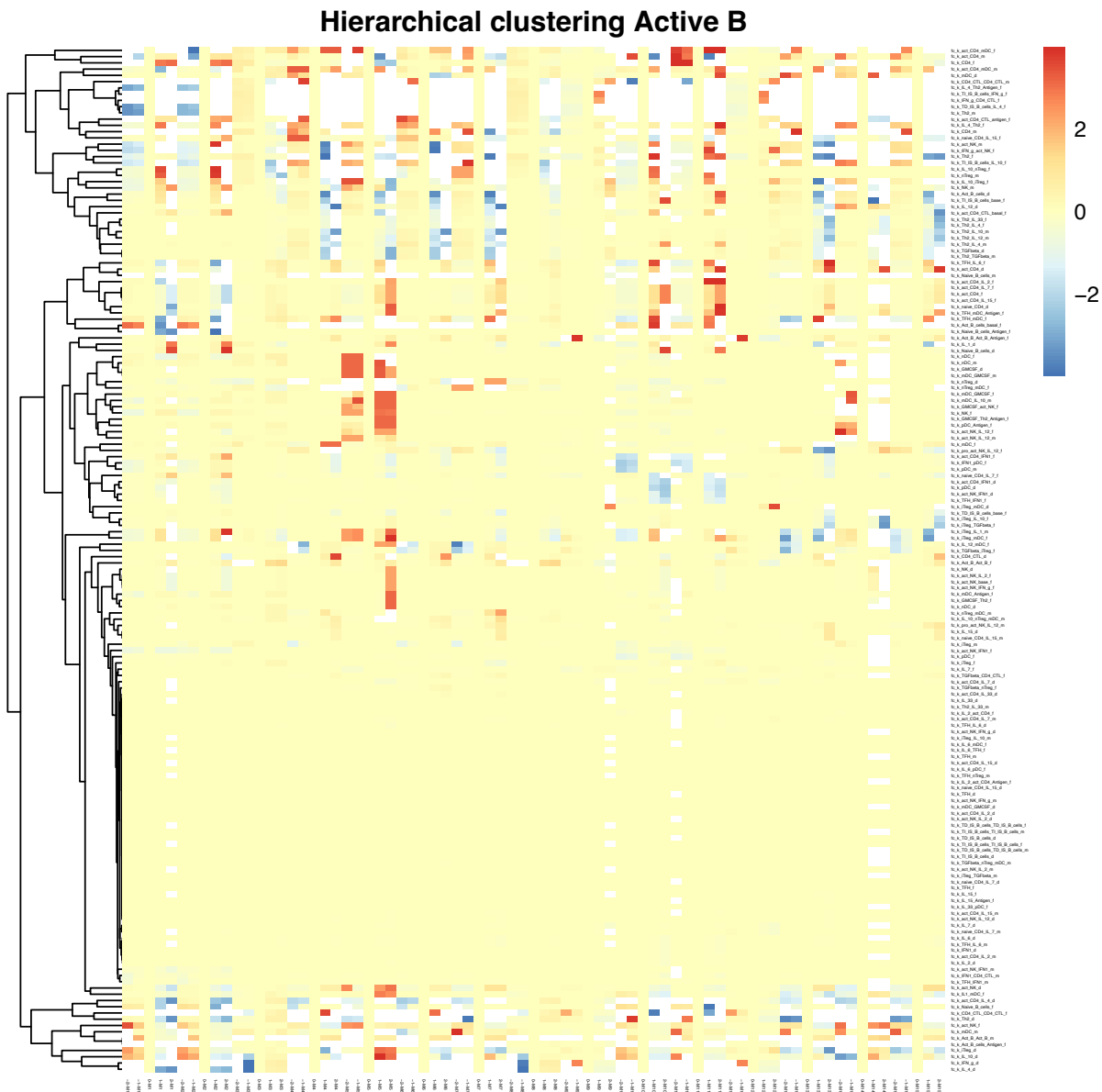


116 **Supplementary Figure 12. Sensitivity analysis of TD-Plasma cells by varying**
 117 **model parameters.** Depicted are changes in active B cell counts upon perturbing the
 118 model parameters, with the change measured as $(\text{cell_count}_{\text{perturbed}} - \text{cell_count}_{\text{original}}) / \text{cell_count}_{\text{original}}$. Each row represents a model parameter. The columns show fold-
 119 changes in respective parameters in each of the 15 model instances, as labeled from M1
 120 to M15.

Hierarchical clustering TI-Plasma

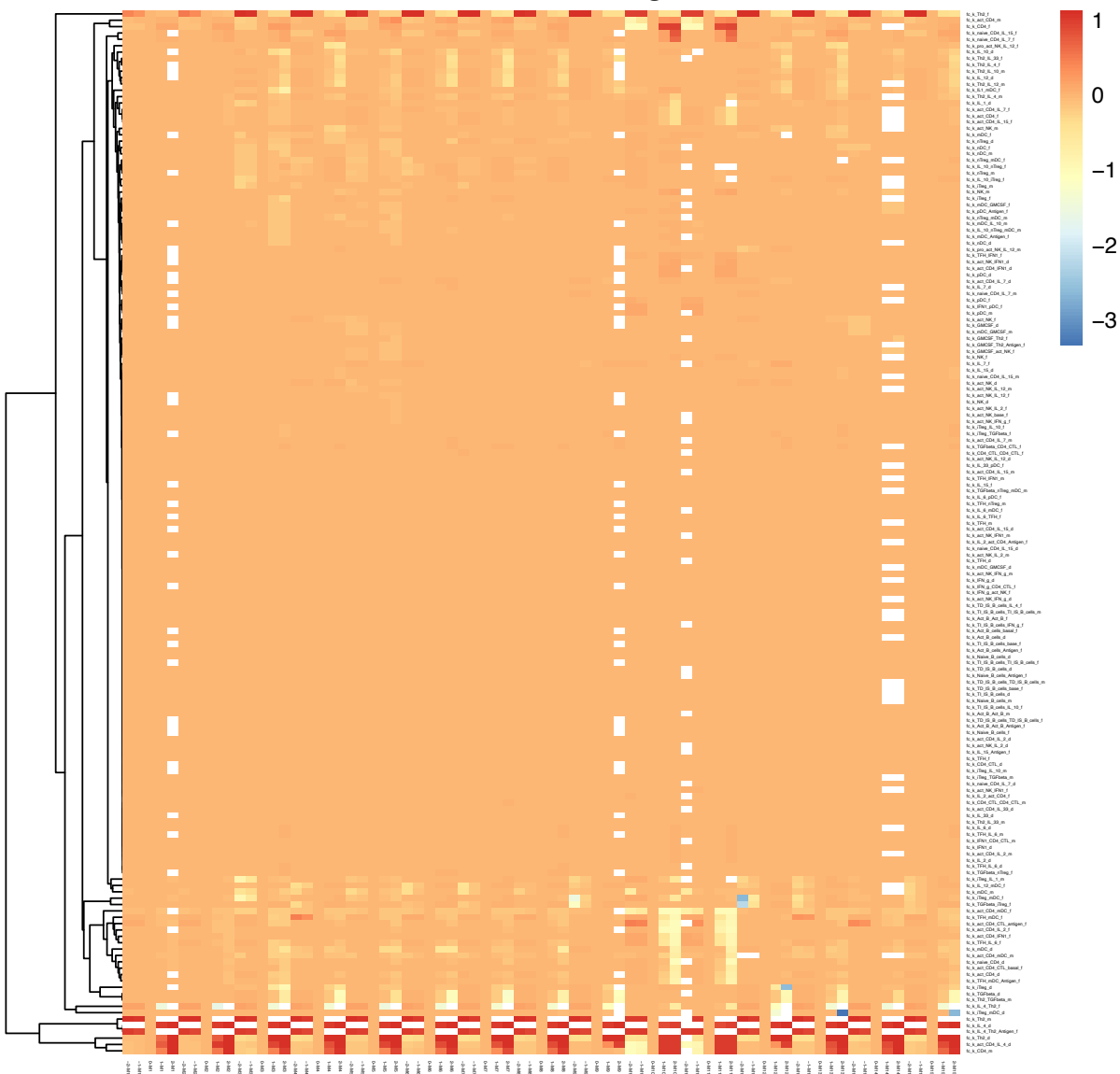


122 **Supplementary Figure 13 Sensitivity analysis of TI-Plasma cells by varying model**
123 **parameters.** Depicted are changes in active B cell counts upon perturbing the model
124 parameters, with the change measured as $(\text{cell_count}_{\text{perturbed}} - \text{cell_count}_{\text{original}}) / \text{cell_count}_{\text{original}}$. Each row represents a model parameter. The columns show fold-
125 changes in respective parameters in each of the 15 model instances, as labeled from M1
126 to M15.



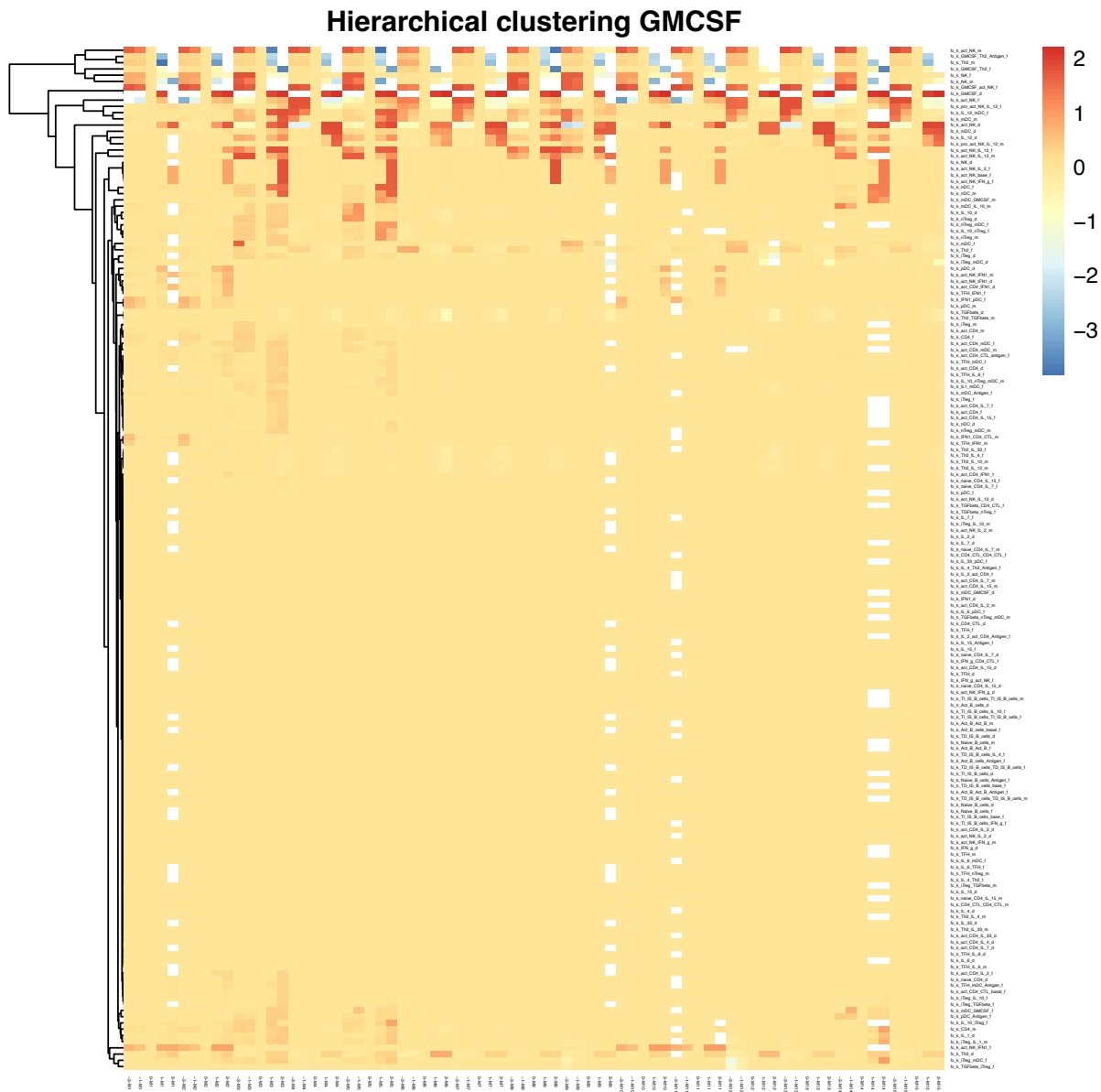
128 **Supplementary Figure 14. Sensitivity analysis of active B cells by varying model**
129 **parameters.** Depicted are changes in active B cell counts upon perturbing the model
130 parameters, with the change measured as $(\text{cell_count}_{\text{perturbed}} - \text{cell_count}_{\text{original}}) / \text{cell_count}_{\text{original}}$. Each row represents a model parameter. The columns show fold-
131 changes in respective parameters in each of the 15 model instances, as labeled from M1
132 to M15.

Hierarchical clustering IL_4



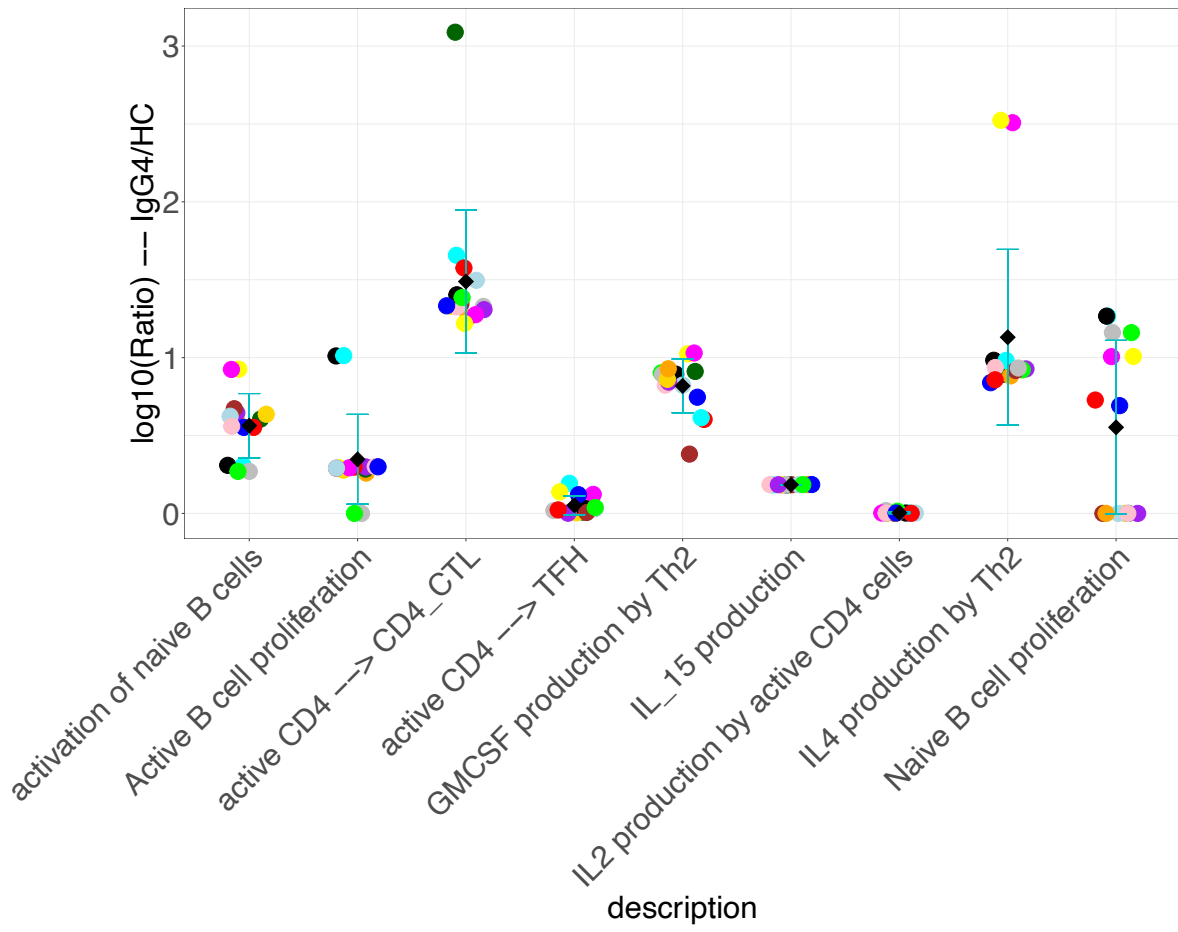
134 **Supplementary Figure 15. Sensitivity analysis of IL-4 by varying model**
135 **parameters.** Depicted are changes in active B cell counts upon perturbing the model
136 parameters, with the change measured as $(\text{cell_count}_{\text{perturbed}} - \text{cell_count}_{\text{original}}) / \text{cell_count}_{\text{original}}$. Each row represents a model parameter. The columns show fold-
137 changes in respective parameters in each of the 15 model instances, as labeled from M1
138 to M15.

139
140

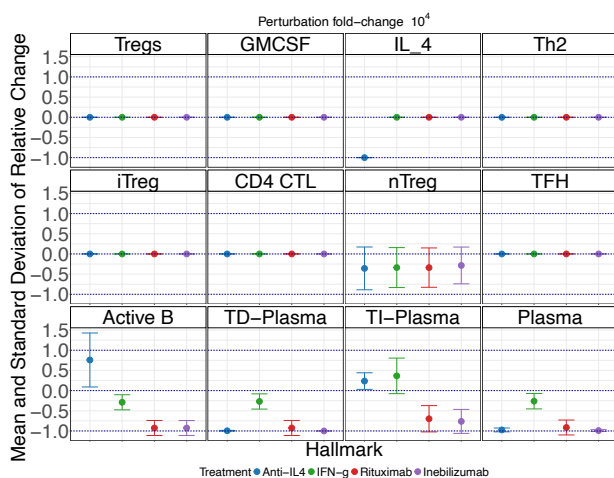
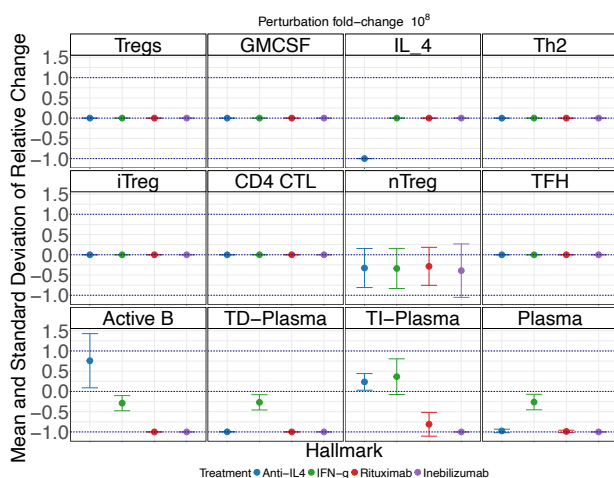
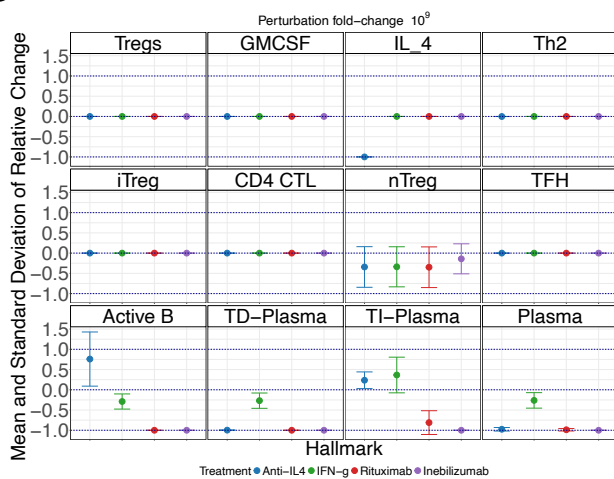


141 **Supplementary Figure 16. Sensitivity analysis of GM-CSF by varying model**
142 **parameters.** Depicted are changes in active B cell counts upon perturbing the model
143 parameters, with the change measured as $(\text{cell_count}_{\text{perturbed}} - \text{cell_count}_{\text{original}}) / \text{cell_count}_{\text{original}}$. Each row represents a model parameter. The columns show fold-
144 changes in respective parameters in each of the 15 model instances, as labeled from M1
145 to M15.

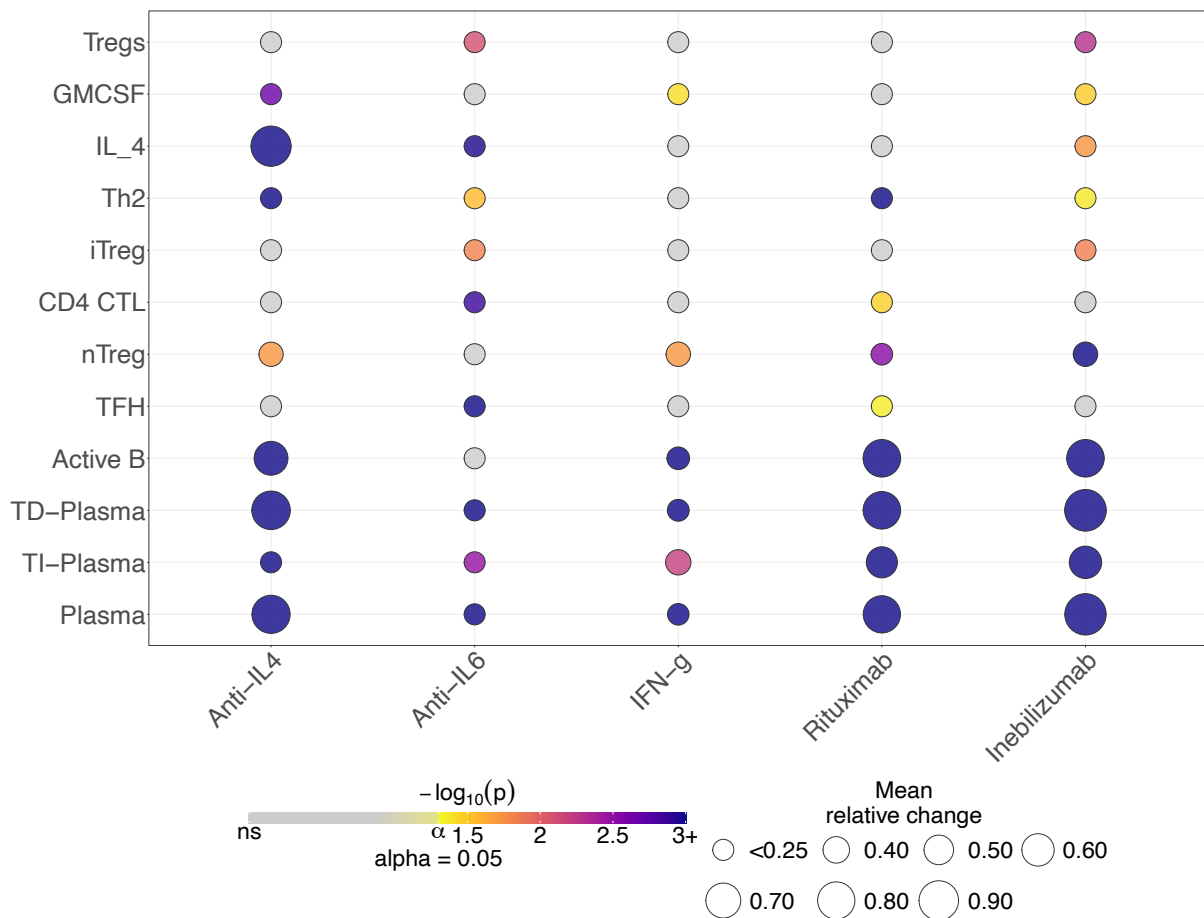
147



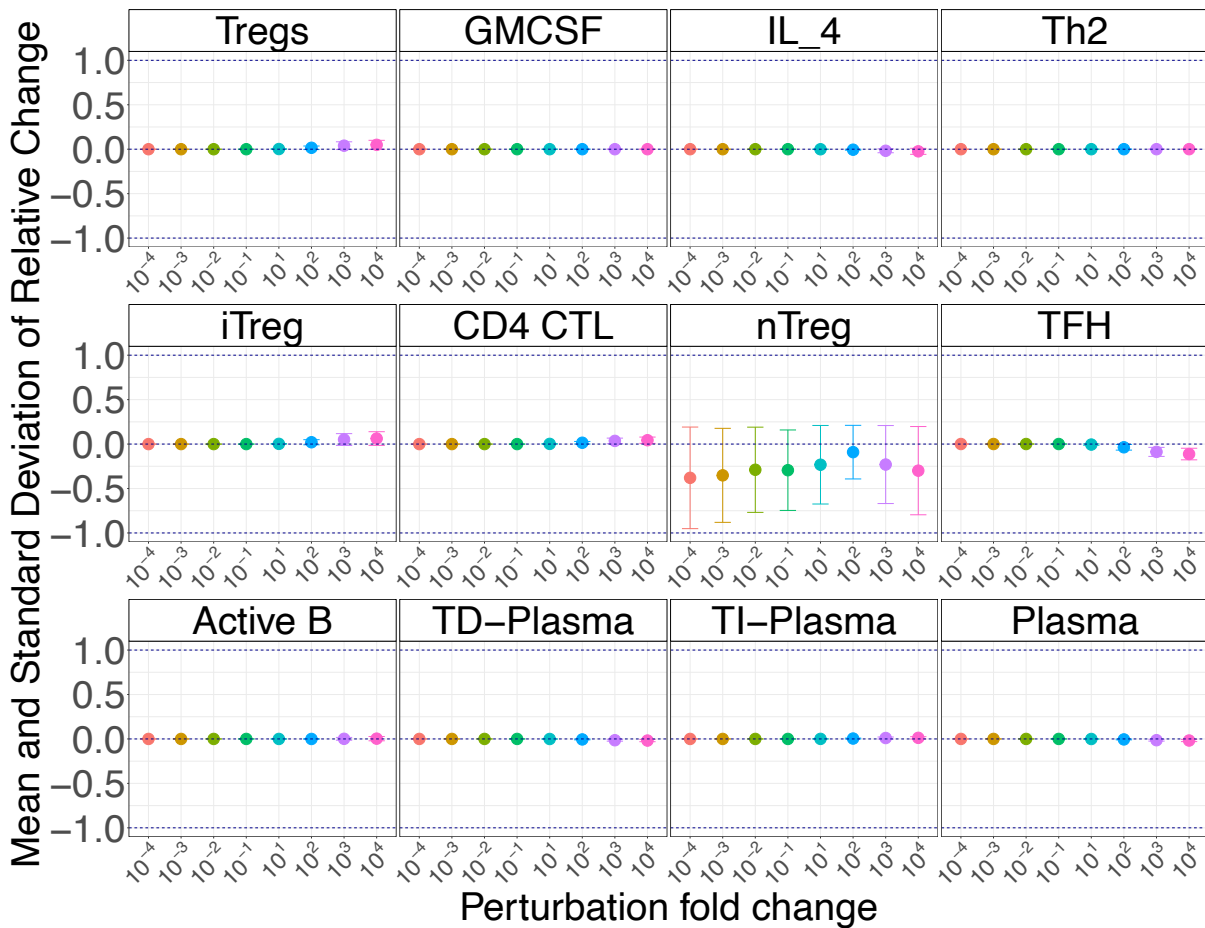
148 **Supplementary Figure 17. Model-inferred changes in differentially regulated**
149 **processes in IgG4-RD patients (IgG4RD) compared to the healthy controls (HC).**
150 The changes are presented in $\log_{10}(\text{IgG4RD}/\text{HC})$ value. Each dot represents one of the
151 15 calibrated instances of the model. In addition, mean and standard deviations are
152 presented.

A**B****C**

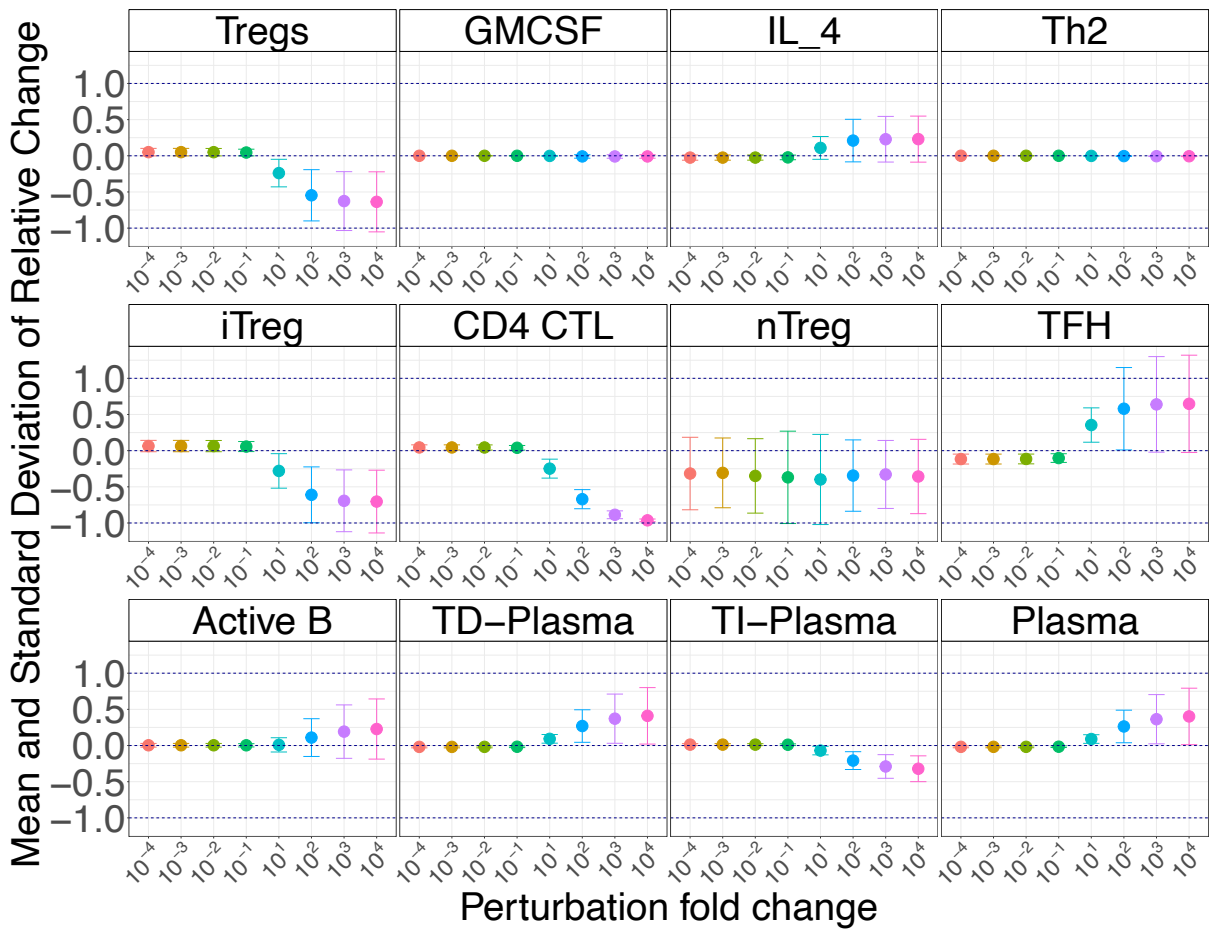
153 **Supplementary Figure 18.** Treatment simulations with varied perturbation
154 strengths corresponding to Figure 6A. Log₁₀ fold-changes of parameters were set in
155 (A) to 4, in (B) to 8, and in (C) to 9.



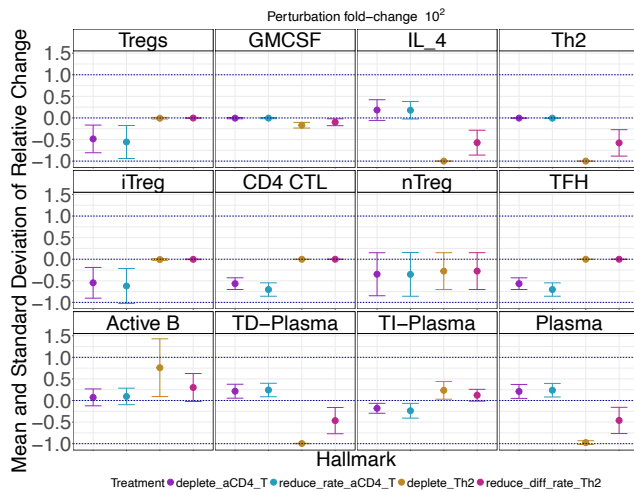
157 **Supplementary Figure 19. Statistical tests of the treatment effects on IgG4-RD**
158 **hallmarks, associated with the *in silico* perturbation experiments in Figure 6A.**
159 Bubble sizes represent mean values of the perturbation effects and the colors represent
160 the P values.



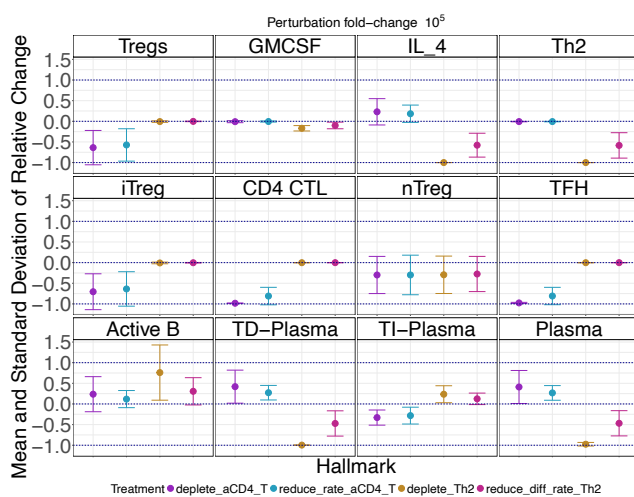
161 **Supplementary Figure 20. Changes of IgG4-RD hallmarks upon *in silico* anti-IL-
162 6 treatment.** Presented are relative changes in cell counts or cytokine levels by post-
163 treatment compared to no treatment, in response to changes in degradation rate of IL-
164 6 in the model. Different colors denote $\log_{10}(\text{fold-change})$ values. Dots: mean values
165 across 15 instances of the model; error bars: standard deviations of the simulated results
166 across 15 instances of the model.



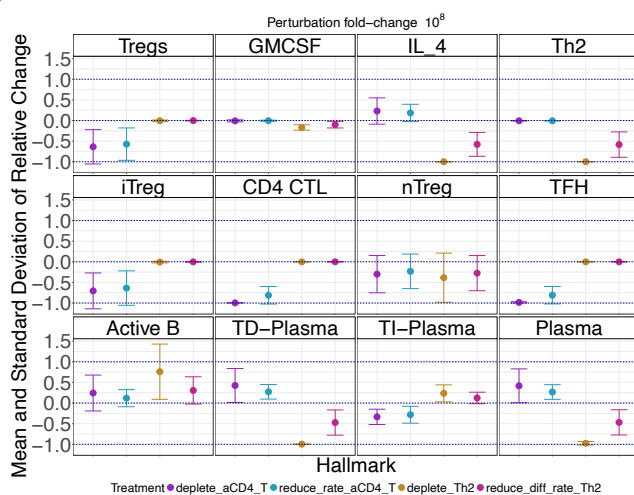
167 **Supplementary Figure 21. Changes of IgG4-RD hallmarks upon *in silico***
168 **perturbation of IL-6-induced T_{FH} differentiation.** Presented are relative changes in
169 cell counts or cytokine levels by post-treatment compared to no treatment in response
170 to changes in the rate of T_{FH} differentiation induced by IL-6. Different colors denote
171 $\log_{10}(\text{fold-change})$ values. Dots: mean values across 15 instances of the model; error
172 bars: standard deviations of the simulated results across 15 instances of the model.



B

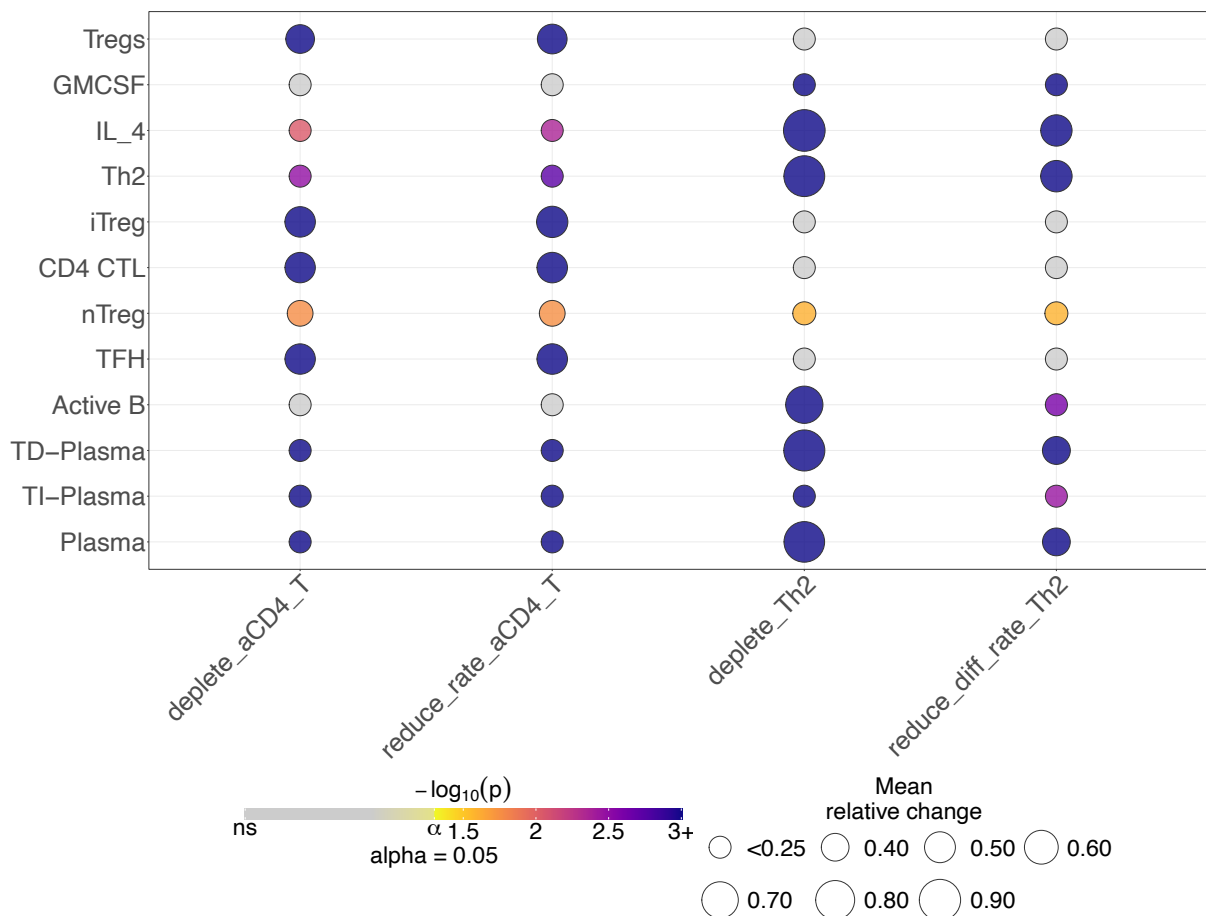


C



173

174 **Supplementary Figure 22. Treatment simulations with varied perturbation**
 175 **strengths corresponding to Figure 6B.** Log₁₀ fold-changes of parameters were set in
 176 (A) to 2, (B) to 5, and (C) to 8.



177 **Supplementary Figure 23. Statistical tests of the treatment effect on IgG4-RD**
178 **hallmarks, associated with the *in silico* perturbation in Figure 6B.** Bubble sizes
179 represent mean values of the perturbation effects and the colors represent the *P* values.

180

Supplementary Table 1. Baseline clinical, imaging, and pathological characteristics of the patients

No.	Sex	Age	Main Symptoms	Associated Symptoms	Multi-system	Organ involvement	Imaging findings	Pathological features	RI*
1	M	64	Bilateral submandibular gland enlargement	Dry mouth and eyes	1	Salivary glands	Diffuse lesions in bilateral parotid glands; enlarged submandibular glands with abnormal echogenicity	Partial acinar atrophy with stromal fibrosis and dense infiltration of lymphomononuclear cells, plasma cells 40-50 IgG4 ⁺ /HPF*, IgG4/IgG > 40%	2
2		58	Jaundice of the skin and sclera	Skin pruritus, upper abdominal discomfort, and a weight loss of 6kg	2	Pancreas, bile ducts	Common bile duct dilatation with distal obstruction; pancreatic swelling with "sausage-like" appearance; capsule-like rim; delayed enhancement; long-segment stenosis of main pancreatic duct	\	4
3	F	72	Weight loss	\	1	Pancreas	Pancreatic head swelling with small enhancing foci; T2WI signal abnormality in pancreatic body	\	2
4	F	72	Elevated ESR*	History of right-sided abdominal discomfort	3	Periarteritis, paravertebral region, kidneys	Soft tissue around pulmonary arteries with homogeneous enhancement; periaortic soft tissue at L3 (periaortitis); multiple low-enhancing renal lesions	\	6
5	M	56	Abdominal pain	Occasional dry mouth and eyes	2	Pancreas, kidneys	Heterogeneous pancreatic echogenicity; bilateral renal morphological and signal abnormalities with uneven cortical enhancement; persistent heterogeneous pancreatic echogenicity after treatment	\	4
6	F	82	Dry mouth and eyes, with edema	Oliguria	5	Bile duct, liver, kidneys, lacrimal	Liver mass; heterogeneous echogenicity in bilateral salivary	Significant fibrous tissue hyperplasia with dense lymphoplasmacytic	6

7	F	39	Lacrimal gland enlargement	\	1	Lacrimal glands	glands; impaired uptake in parotid and submandibular glands; increased renal arterial resistance index Bilateral dacryoadenitis; multiple lymphadenopathies in mediastinum and axilla
8	M	50	Enlargement of the parotid and lacrimal glands	\	1	Parotid glands	Swelling of parotid, submandibular, and lacrimal glands with multiple hypoechoic areas

* RI: IgG4-RD Responder Index.

* HPF: high power field microscopy. Here refers to the number of IgG4⁺ plasma cells under the high-power field microscopy.

* ESR: erythrocyte sedimentation rate.

1 **Supplementary Table 2. Multi-omic measurements by patients.**

ID	Age	Gender	scRNaseq	Flow	MSD
1	64	Male			
2	58	Male			
3	72	Female			
4	72	Female			
5	56	Male			
6	82	Female			
7	39	Female			
8	50	Male			

2

3

ID	Age	Gender	Lab tests	scRNaseq	Flow	MSD
Patient-1	64	Male	✓	✓	✗	✗
Patient-2	58	Male	✓	✓	✗	✓
Patient-3	72	Female	✓	✓	✓	✓
Patient-4	72	Female	✓	✓	✓	✓
Patient-5	56	Male	✓	✓	✓	✓
Patient-6	82	Female	✓	✓	✗	✓
Patient-7	39	Female	✓	✓	✓	✓
Patient-8	50	Male	✓	✓	✓	✓
Control-1			✓			
Control-2			✓			
Control-3			✓			
Control-4			✓			
Control-5			✓			
Control-6			✓			
Control-7			✓			
Control-8			✓			
Control-9			✓			

4

5 **Supplementary Table 3. Antibodies used for flow cytometry.**

Antigen	Clone	Dilution	Fluorochrome	Supplier
CD45	HI30	1:20	PerCP-Cy5.5	BD Biosciences
BD Multi-test 6-color TBNK (CD3, CD16 ⁺⁵⁶ , CD45, CD4, CD19, CD8)	/	1:10	FITC/PE/PerCP-Cy5.5/PC7/APC/APC-Cy7	BD Biosciences
CD4	SK3	1:50	PE-Cy7	BD Biosciences
CD8	SK1	1:50	APC-Cy7	BD Biosciences
CD4	RPA-T4	1:50	FITC	BD Biosciences
CD127	HIL-7R-M21	1:50	PE	BD Biosciences
CD25	M-A251	1:50	APC	BD Biosciences
Lineage Cocktail 1 (CD3, CD14, CD16, CD19, CD20, CD56)	/	1:20	FITC	BD Biosciences
HLA-DR	G46-6	1:50	BV421	BD Biosciences
CD45RO	UCHL1	1:20	PE	BD Biosciences
CD45RA	HI100	1:20	APC	BD Biosciences
CD3	HIT3a	1:50	FITC	BD Biosciences

7 **Supplementary Table 4. Cytokines quantified by the Meso Scale Discovery**
8 **proteomics platform.**

Test Kit	Marker
BOX-1	GM-CSF, IFN- γ , IL-17A, IL-1 β , IL-2, IL-4, IL-5, IL-6, IL-8, IL-10
BOX-2	IL-12p70, IL-13, TNF- α , VEGF-A, ENA-78, IL-33, IL-1RA, IL-2R α , IL-3, Eotaxin-2
BOX-3	Eotaxin, IP-10, MCP-1, MCP-4, MDC, MIP-1 α , MIP-1 β , TARC, MIP-3 α
BOX-4	SDF-1 α , G-CSF, IL-1 α , IL-7, IL-15, IL-16, TNF- β , IL-12/IL-23p40
BOX-5	MIF, MIP-5

9

10 **Supplementary Table 5. scRNA-seq datasets of PBMCs for healthy controls.**

Sample Name	Raw Sample Name	Age	Sex	Access ion	Project	Publication	Project Details
B3_74_M	C3	74	Male	GSM5335492	GSE175499	https://doi.org/10.1016/j.celrep.2021.110039	27 PBMC samples from 15 SFTS patients (including four deceased and 11 surviving) and four healthy controls
B4_70_F	C4	70	Female	GSM5335493	GSE175499	https://doi.org/10.1016/j.celrep.2021.110039	27 PBMC samples from 15 SFTS patients (including four deceased and 11 surviving) and four healthy controls
B5_52_M	PBMC_healthy [52BA2 3-00]	52	Male	GSM5227130	GSE171555	10.1016/j.medj.2021.04.008	PBMC samples from healthy person
B6_61_M	PBMC_healthy [655A9 1-00]	61	Male	GSM5227134	GSE171555	10.1016/j.medj.2021.04.008	PBMC samples from healthy person
B13_U_U	Control -1	>60	Unknown	GSM4497125	GSE149313	https://doi.org/10.1128/mbio.02583-20	PBMC from Control, Infection, Recovery and Fatal patients of Severe fever with thrombocytopenia syndrome banyangvirus

B15_U_U	Control	> 6 0	Unk now n	GSM4 49712 7	GSE1 4931 3	https://doi.org/10.1128/mbio.02583-20	PBMC from Control, Infection, Recovery and Fatal patients of Severe fever with thrombocytopenia syndrome banyangvirus
---------	---------	-------	-----------	--------------	-------------	---	---

11

12 **Supplementary Table 6. Processes with differential interaction rates for IgG4-**
 13 **RD compared with the healthy control state.**

Process	Description
Differentiation of DC cells into pDC cells	These processes are stimulated by the antigen and only occur in the disease state.
Differentiation of DC cells into mDC cells (basal and induced by GMCSF)	
Activation of naïve B cells	
Naïve B cell proliferation	
Active B cell proliferation	
Differentiation of active CD4 T cells into T_{FH} cells	These processes occur with different rates in healthy and disease states.
Differentiation of active CD4 T cells into CD4 CTL	
IL-2 production by active CD4 T cells	
IL-4 production by T_{H2} cells	
GM-CSF production by T_{H2} cells	
IL-15 production	

14

15 **Supplementary Table 7. Model parameter values in the disease state inferred by**
 16 **fitting the IgG4-RD disease model to multi-omic data.** The mean and standard
 17 deviation of the estimated parameter values across the 15 calibrated instances of the
 18 model are listed.

unit	Parameter name	mean	Standard deviation
1/time	k_IFN_g_CD4_CTL_f	22978.01	17070.54
1/time	k_GMCSF_Th2_Antigen_f	3053.59	2477.62
1/time	k_IL_10_nTreg_f	2774.48	5306.99
1/time	k_IL_4_Th2_Antigen_f	1721.09	756.54
1/time	k_TI_IS_B_cells_d	860.77	2271.49
1/time	k_Naive_B_cells_Antigen_f	814.14	1291.61
1/time	k_IL_6_mDC_f	654.92	884.03
1/time	k_IL_6_TFH_f	490.47	612.03
1/time	k_IL_12_mDC_f	478.06	1224.31
1/time	k_IL_2_act_CD4_Antigen_f	443.38	479.62
1/time	k_IL_33_pDC_f	416.88	614.37
1/time	k_IL_6_pDC_f	270.62	351.16
1/time	k_TI_IS_B_cells_TI_IS_B_cells_f	266.02	364.51
1/time	k_Act_B_Act_B_Antigen_f	149.55	314.95
1/time	k_mDC_GMCSF_f	94.6	278.73
1/time	k_nDC_f	86.9	274.42
1/time	k_act_CD4_IL_7_d	55.56	37.12
1/time	k_act_CD4_mDC_f	39.54	99.5
1/time	k_IFN_g_act_NK_f	34.31	27.11
1/time	k_naive_CD4_IL_7_f	22.35	59.09
1/time	k_IL_2_d	16.72	18.1
1/time	k_TD_IS_B_cells_d	15.46	17.38
1/time	k_IL_10_iTreg_f	14.1	22.05
1/time	k_pro_act_NK_IL_12_f	12	30.27
1/time	k_GMCSF_act_NK_f	11.37	12.6
1/time	k_mDC_Antigen_f	8.5	13.73
1/time	k_pDC_Antigen_f	7.92	12.12
1/time	k_mDC_d	3.17	10.01
1/time	k_IL1_mDC_f	3.03	2.13
1/time	k_CD4_f	2.75	6.69
1/time	k_naive_CD4_IL_15_f	2.68	4.41
1/time	k_pDC_d	2	6.52

1/time	k_Act_B_cells_Antigen_f	1.69	1.23
1/time	k_iTreg_mDc_f	1.21	2.17
1/time	k_NK_f	1.2	2.28
1/time	k_IgG4_TD_IS_B_cells_f	1	0
1/time	k_IgG4_TI_IS_B_cells_f	1	0
1/time	k_TFH_f	1	0
1/time	k_act_NK_IL_12_f	0.96	1.76
1/time	k_GMCSF_d	0.83	0.94
1/time	k_iTreg_d	0.57	1.33
1/time	k_nTreg_d	0.51	0.69
1/time	k_TFH_mDc_Antigen_f	0.3	0.37
1/time	k_nTreg_mDc_f	0.3	0.58
1/time	k_IL_6_d	0.28	0.33
1/time	k_act_CD4_CTL_antigen_f	0.25	0.57
1/time	k_IL_10_d	0.23	0.39
1/time	k_act_NK_d	0.23	0.58
1/time	k_IL_4_d	0.19	0.2
1/time	k_CD4_CTL_CD4_CTL_f	0.13	0.2
1/time	k_act_NK_IFN1_f	0.13	0.14
1/time	k_IFN1_pDC_f	0.12	0.15
1/time	k_Th2_f	0.12	0.09
1/time	k_act_CD4_IL_4_d	0.12	0.09
1/time	k_IL_12_d	0.11	0.17
1/time	k_iTreg_TGFbeta_f	0.11	0.21
1/time	k_TGFbeta_iTreg_f	0.09	0.13
1/time	k_CD4_CTL_d	0.08	0.07
1/time	k_IFN_g_d	0.07	0.05
1/time	k_IFN1_d	0.06	0.06
1/time	k_TFH_IFN1_f	0.06	0.06
1/time	k_TFH_IL_6_f	0.06	0.05
1/time	k_TGFbeta_CD4_CTL_f	0.06	0.06
1/time	k_TGFbeta_d	0.06	0.05
1/time	k_Th2_IL_4_f	0.06	0.05
1/time	k_act_CD4_IFN1_d	0.06	0.06
1/time	k_act_CD4_IL_15_d	0.06	0.05
1/time	k_act_NK_IFN1_d	0.06	0.06
1/time	k_act_NK_IFN_g_d	0.06	0.06

1/time	k_iTreg_mDC_d	0.06	0.05
1/time	k_mDC_GMCSF_d	0.06	0.06
1/time	k_naive_CD4_IL_15_d	0.06	0.06
1/time	k_naive_CD4_IL_7_d	0.06	0.05
1/time	k_naive_CD4_d	0.06	0.12
1/time	k_Act_B_cells_d	0.05	0.04
1/time	k_IL_15_d	0.05	0.01
1/time	k_IL_33_d	0.05	0.07
1/time	k_TFH_IL_6_d	0.05	0.06
1/time	k_TGFbeta_nTreg_f	0.05	0.06
1/time	k_Th2_IL_33_f	0.05	0.04
1/time	k_act_CD4_IFN1_f	0.05	0.05
1/time	k_act_CD4_IL_2_d	0.05	0.06
1/time	k_act_CD4_IL_33_d	0.05	0.05
1/time	k_act_CD4_IL_7_f	0.05	0.11
1/time	k_act_NK_IL_12_d	0.05	0.06
1/time	k_act_NK_IL_2_d	0.05	0.06
1/time	k_TD_IS_B_cells_base_f	0.04	0.03
1/time	k_act_CD4_d	0.04	0.03
1/time	k_act_NK_f	0.04	0.03
1/time	k_iTreg_IL_10_f	0.04	0.03
1/time	k_IL_7_d	0.03	0.03
1/time	k_Naive_B_cells_d	0.03	0.02
1/time	k_TFH_d	0.03	0.03
1/time	k_Th2_d	0.03	0.03
1/time	k_act_CD4_IL_2_f	0.03	0.02
1/time	k_act_CD4_IL_15_f	0.02	0.02
1/time	k_act_CD4_f	0.02	0.02
1/time	k_IL_1_d	0.01	0
1/time	k_NK_d	0.01	0.03
1/time	k_TD_IS_B_cells_TD_IS_B_cells_f	0.01	0.01
1/time	k_act_NK_IFN_g_f	0.01	0.01
1/time	k_act_NK_IL_2_f	0.01	0.02
1/time	k_act_NK_base_f	0.01	0.01
1/time	k_nDC_d	0.01	0.01
1/time	k_TD_IS_B_cells_IL_4_f	0	0
1/time	k_TD_IS_B_cells_base_f	0	0

1/time	k_TI_IS_B_cells_IFN_g_f	0	0
1/time	k_TI_IS_B_cells_IL_10_f	0	0
1/time	k_iTreg_f	0	0
1/(μl*time)	k_IL_7_f	24750.2	20450.11
1/(μl*time)	k_IL_15_Antigen_f	7547.31	957.75
1/μl	k_naive_CD4_IL_7_m	117927.9	311254.62
		7	
1/μl	k_mDc_IL_10_m	67190.33	196717.83
1/μl	k_act_CD4_IL_7_m	21639.64	29705.15
1/μl	k_pro_act_NK_IL_12_m	14800.21	52545.39
1/μl	k_act_NK_IL_12_m	12749.46	13570.68
1/μl	k_act_NK_IL_2_m	880.36	866.61
1/μl	k_act_CD4_IL_2_m	709.93	810.27
1/μl	k_Th2_IL_33_m	583.55	598.69
1/μl	k_act_CD4_IL_15_m	580	587.19
1/μl	k_act_NK_IFN_g_m	573.6	565.57
1/μl	k_naive_CD4_IL_15_m	516.94	555.56
1/μl	k_Th2_IL_4_m	472.39	556.06
1/μl	k_Th2_IL_12_m	466.53	333.69
1/μl	k_mDc_GMCSF_m	461.37	553.13
1/μl	k_Th2_IL_10_m	429.92	259.37
1/μl	k_iTreg_IL_10_m	419.03	263.25
1/μl	k_Tfh_IL_6_m	418.36	348.61
1/μl	k_act_NK_m	326.73	169.31
1/μl	k_act_CD4_m	270.21	3.87
1/μl	k_CD4_m	207.64	7.15
1/μl	k_Naive_B_cells_m	105.32	21.58
1/μl	k_iTreg_IL_1_m	100.75	112.27
1/μl	k_Act_B_Act_B_m	86.78	4.71
1/μl	k_act_CD4_mDc_m	67.2	162.58
1/μl	k_NK_m	59.33	7.19
1/μl	k_iTreg_m	39.82	23.17
1/μl	k_nDc_m	35.85	2.47
1/μl	k_mDc_m	33.59	38.27
1/μl	k_nTreg_m	13.85	22.91
1/μl	k_pDc_m	7.24	5.27
1/μl	k_IL_10_nTreg_mDc_m	2.54	7.18

1/ μ l	k_TD_IS_B_cells_TD_IS_B_cells_m	1.09	0.45
1/ μ l	k_TFH_m	0.28	0.22
1/ μ l	k_Th2_m	0.28	0.16
1/ μ l	k_TI_IS_B_cells_TI_IS_B_cells_m	0.18	0.34
1/ μ l	k_TFH_nTreg_m	0.16	0.21
1/ μ l	k_nTreg_mDCC_m	0.16	0.17
1/ μ l	k_IFN1_CD4_CTL_m	0.06	0.05
1/ μ l	k_TFH_IFN1_m	0.06	0.05
1/ μ l	k_TGFbeta_nTreg_mDCC_m	0.06	0.06
1/ μ l	k_act_NK_IFN1_m	0.06	0.06
1/ μ l	k_iTreg_TGFbeta_m	0.06	0.06
1/ μ l	k_Th2_TGFbeta_m	0.04	0.02
1/ μ l	k_CD4_CTL_CD4_CTL_m	0.03	0.02

Process	p-value
Differentiation of DC cells into pDC cells	-
Differentiation of DC cells into mDC cells (basal and induced by GMCSF)	-
Activation of naïve B cells	0.01
Naïve B cell proliferation	0.1
Active B cell proliferation	0.3
Differentiation of active CD4 T cells into TFH cells	0.5
Differentiation of active CD4 T cells into CD4 CTL	< 0.01
IL-2 production by active CD4 T cells	0.7
IL-4 production by T _H 2 cells	< 0.01
GMCSF production by T _H 2 cells	< 0.01
IL-15 production	< 0.01

20